UNIVERSITE DE NEUCHATEL FACULTE DES SCIENCES

ETUDE PAR SECTROSCOPIE D'ELECTRONS DES COUCHES f INCOMPLETES DANS LES SOLIDES

FORME REDUITE DE LA THESE

présentée à la Faculté des Sciences
pour l'obtention du grade de docteur ès sciences
de l'Université de Neuchâtel
par

Eric Wuilloud
Physicien diplômé

IMPRIMATUR POUR LA THÈSE

Etude par spectroscopie d'électrons des couches f incomplètes dans les solides

de M*onsieur Eric Wuilloud*

UNIVERSITÉ DE NEUCHATEL

FACULTÉ DES SCIENCES

La Faculté des sciences de l'Université de Neuchâtel, sur le rapport des membres du jury,

MM. les professeurs Y. Baer, P. Martinoli, H. Beck et P. Wachter (Zurich)

autorise l'impression de la présente thèse.

Neuchâtel, le *4 décembre 1985*

Le doyen:

François Sigrist

François Sigrist

PUBLICATIONS QUI CONTIENNENT L'ESSENTIEL DE LA THESE

Wuilloud E., Baer Y., Maple M.B. 1883 Phys. Lett. 97A 65

Wuilloud E., Moser H.R., Schneider W.D., Baer Y. 1983 Phys. Rev. B 28 7354

Wuilloud E., Baer Y., Ott H.R., Fisk Z., Smith J.L. 1984 Phys. Rev. B 29 5228

Wuilloud E., Schneider W.D., Delley B., Baer Y., Hulliger F. 1984 J. Phys. C: Solid State Phys. 17 4799

Schneider W.D., Wuilloud E., Delley B., Baer Y. 1985 Physica 130B 144

Wuilloud E., Delley B., Schneider W.D., Baer Y. 1984 Phys. Rev. Lett. 53 202

Wuilloud E., Delley B., Schneider W.D., Baer Y. 1984 Phys. Rev. Lett. 53 2519

Wuilloud E., Delley B., Schneider W.D., Baer Y. 1985 J. Magn. Magn. Mat. 47 & 48 197

Schneider W.D., Delley B., Wuilloud E., Imer J.M., Baer Y. 1985 Phys. Rev. B 32 6819

Le texte complet de la thèse est déposé à la bibliothèque de l'Université de Neuchâtel ainsi qu'à la bibliothèque de l'institut de physique de cette Université.

EVIDENCE FOR THE TETRAVALENCE OF CERIUM IN $CeRu_2$ ☆

E. WUILLOUD, Y. BAER
Institut de Physique, Université de Neuchâtel, CH - 2000 Neuchâtel, Switzerland

and

M.B. MAPLE
Institute for Pure and Applied Physical Sciences, University of California, San Diego, La Jolla, CA 92093, USA

Received 3 February 1983
Revised manuscript received 3 June 1983

The conventional analysis of XPS core level spectra of $CeRu_2$ yields a picture of the 4f states which is difficult to reconcile with other results. The validity of this kind of interpretation urgently needs to be re-examined critically. In contrast, Bremsstrahlung isochromat spectroscopy (BIS) measurements on $CeRu_2$, reported herein, suggest that Ce is nearly tetravalent $4f^0$ configuration) in this compound.

The electronic structure of Ce has recently been the subject of numerous experimental and theoretical studies [1–3], but one has to admit that no concensus has emerged as yet. Even the fundamental question of the occupation and energy of the 4f levels in Ce is still a matter of debate and has yet to be resolved. The pictures of the electronic states deduced from different types of observations (thermochemical data, spectroscopic results, atomic volume, magnetism, superconductivity) are hard to reconcile. A typical example of this confusing situation is provided by $CeRu_2$.

A few years ago, the absence of a local moment, the collapsed atomic volume and the superconductivity observed in this compound were considered as symptoms revealing unambiguously the $4f^0$ configuration (tetravalence) of Ce ions in $CeRu_2$ [4,5]. However, only a few of the more recent studies have yielded information supporting this view. It has been predicted by a thermodynamical cycle that the energy of this metallic compound is lower for tetravalent Ce than for trivalent Ce [6]. Mössbauer spectra of ^{99}Ru in XRu_2 (X= La, Ce, Pr, Th) show a single absorption line except for $CeRu_2$ and $ThRu_2$ where a doublet is observed [7]. This is attributed to a quadrupole splitting revealing a much larger electric field gradient at the Ru sites produced by the tetravalent Ce and Th atoms than by the other trivalent rare earth atoms.

On the other hand, the Ce atomic radius in this compound is comparable to that of γ-Ce which is at least accepted to be not tetravalent. For this reason an intermediate valence between 3^+ and 4^+ has been assumed in $CeRu_2$ [1,8]. Born–Haber cycles applied to many Ce compounds including $CeRu_2$ lead to the conclusion that a simple description of the valence of Ce is not compatible with the available thermochemical data [9]. It is assumed that the 4f states contain a part with itinerant character that contributes to the cohesion in all compounds traditionally considered to be tetravalent. Systematic studies of Ce L_{II} and L_{III} absorption edges have been diversely interpreted: they have been claimed (a) to reveal a fractional valence excluding the existence of pure 4^+ states in all compounds expected to be tetravalent (even in CeO_2 !) [10], (b) to be inadequate for differentiating tetravalent from mixed valent Ce ions [11] and, finally (c) to provide

☆ This work is supported at the Physics Institute of Neuchâtel by the Swiss National Science Foundation and at the University of California, San Diego, by the U.S. Department of Energy under Contract No. DE-AT03-76ER70227.

0.031-9163/83/0000–0000/$ 03.00

a suitable tool for distinguishing the different valences of Ce [12,13]. Resonant photoemission spectra of $CeAl_3$ and $CeRu_2$ have been recently compared [14]. The similarity of the behaviour of the structures attributed to 4f states is found to be unmistakable so it is suggested that $CeRu_2$ may be mixed valent.

The discrepancies and uncertainties affecting the different predictions of the 4f population in $CeRu_2$ can be considered as a typical example of the rather systematic lack of consistency emerging from the numerous Ce compound studies. The aim of the present letter is to show by comparing data of $CeRu_2$ to those of other compounds that even if core level spectroscopies yield misleading results, a spectroscopy populating exclusively the levels which are unoccupied in the ground state appears to provide unambiguous information about the 4f shell occupation.

The polycrystalline $CeRu_2$ sample, which was prepared by arc melting, was the same one used in a recent resonant photoemission study [14]. Clean surfaces were obtained in situ by scrapping with an Al_2O_3 file as often as necessary in order to eliminate from the outer level spectra the intensity which was found to be correlated with an increase of the contamination monitored by XPS core levels. Surprisingly, oxygen contamination on the surface was found to accumulate much faster than expected in a surrounding vacuum better than 10^{-11} Torr. We attribute this observation to the diffusion of dissolved oxides from the bulk. The combined XPS-BIS apparatus has been described previously [15,16]. Fig. 1 shows a comparison of the Ce 3d core level spectra of $CeRu_2$, $CePd_3$, and γ-Ce. In the lower part, a computer fit (full line) of the spectrum of $CePd_3$ [17] has been superimposed in order to emphasize their similarity. The evolution of the background toward higher binding energies is not quite identical but the intensity ratios of the different structures do not show pronounced differences. This kind of spectrum is currently observed for any sample supposed to contain tetravalent or mixed valent Ce atoms. Its most characteristic feature is the presence of two peaks (A) usually interpreted as $3d^9_{3/2,5/2}4f^0$ final states and roughly separated by 10 eV from the structures (B) attributed to the $3d^94f^1$ multiplet final states. This energy separation between final states with different 4f populations is correctly predicted by renormalized-atom calculations [18]. More detailed analysis of such spectra [19] have been proposed where, in addition, the structures (C) have been attributed to $3d^94f^2$ final states. Qualitatively, this description seems to be quite satisfactory but it raises a very puzzling question. It is wel established that XPS core level spectra do not reflect quite faithfully the initial configuration but no convincing explanation can be found for the fact that the XPS structures (A), commonly assigned to the $3d^94f^0$ final states, have usually a very weak intensity when compared to other structures. A theoretical calculation taking into account the hybridization between f and conduction electrons has been performed in order to predict the probabilities of the different final state configurations in core level XPS spectra [20]. Within this framework the 4f degeneracy is neglected, a rather extreme hybridization is necessary to explain the spectra of $CePd_3$. If this type of interpretation is correct, one obviously has to conclude that Ce also has a mixed valence in $CeRu_2$. Another theoretical approach [21] in the infinite 4f degeneracy limit yields results which agree with the 3d spectrum of $CeRu_2$ when a hybridization energy of 0.1 eV and an initial 4f population of about 0.8 are assumed. In this connection it is interesting to consider the situation encountered in the 3d and 4d spectra of CeO_2 [22] where the peaks traditionally

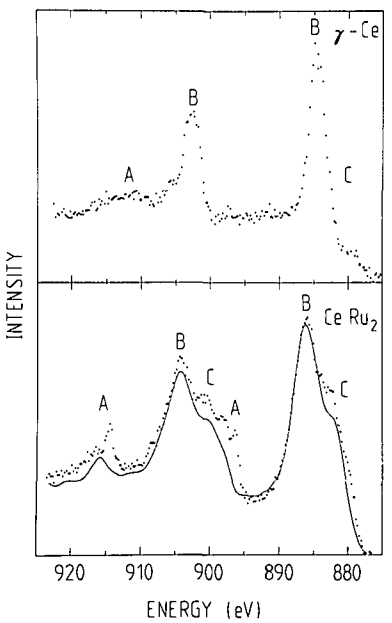

Fig. 1.

interpreted as accounting for $4f^0$ final states represent less than half the total intensity. One could conclude that CeO_2 is mixed valent but this seems unlikely [23]. The cluster calculations performed for analyzing the XPS spectra of CeO_2 [22] yield energies not exceeding 2.15 eV for O 2p → Ce 4f shake-up processes. The remaining high binding energy peaks have been tentatively interpreted as 5p → *n*p excitations. A comparison of 3d XPS and ELS spectra of $CeRu_2$ plotted on a common energy scale shows that the assignment of the different peaks observed by these two techniques is by far not obvious [24] ‡1. It has also been observed that the temperature dependence of the intensity distribution among the diffent peaks of 3d and 4d spectra of $CePd_3$ predicts that Ce becomes purely trivalent at low temperature [25]. This result is completely at variance with the valence changes deduced from all other techniques. A careful investigation of the trend of these 3d spectra for decreasing temperature reveal a striking increase of the intensity ratio of the main peak to the satellite structure (labelled B and C in the spectra of $CeRu_2$ and $CePd_3$, fig. 1). In γ-Ce, the strong peak (B) is commonly attributed to the $4f^1$ configuration, as expected in the sudden approximation, and the weak peak (C) to a $4f^2$ final state resulting from a shake-down process. It is also worth noting that the 3d spectrum of γ-Ce contains flat structures (A) of sizable intensity between 908 and 915 eV which can also be observed in the spectra of other authors [19]. Their presence can call into question the existence of a pure $4f^1$ initial configuration of the fact that a $4f^0$ initial configuration can be unambiguously revealed by some intensity in that region of the spectra. At the present time it does not seem possible to reconcile all these contradictory observations.

Let us now consider the spectra of fig. 2 accounting for direct emission (XPS) or occupation (BIS) of the states around the Fermi energy. Such XPS spectra (left panel) have already been discussed at great length [17]. The main difficulty encountered in their interpretation arises from the low occupation and the relatively mod-

‡1 The 3d ELS spectrum of Ce (supposed to be nearly tetravalent in $CeRu_2$) can be expected to account essentially for $3d^9 4f^1$ final states. In fact it does not contain any indication of the main XPS 3d peaks (B), but shows only structures coinciding perfectly with the structures (C) in fig. 1.

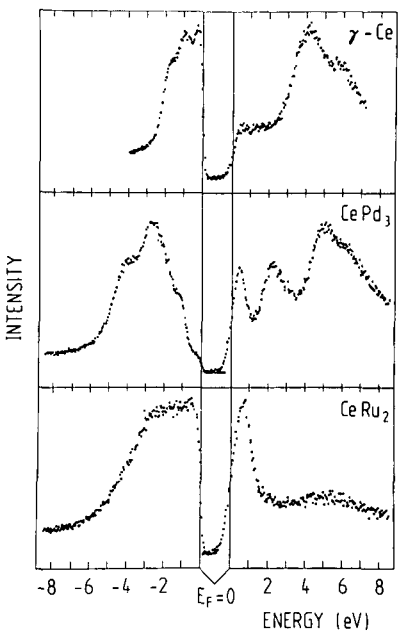

Fig. 2.

est photoionization cross-section of the 4f states compared with those of band states of other symmetries. Even in the XPS spectrum of γ-Ce which offers the most favourable situation, an unambiguous assignment of one of the structures to the emission of the $4f^1$ state remains somewhat hazardous. In the compounds, any identification becomes impossible without comparison with the spectra of the corresponding lanthanum compound. On the contrary, the density of unoccupied states in a small energy range above E_F is dominated by the nearly or completely empty 4f shell. Therefore, it is much easier to investigate the valence of Ce by electronic processes increasing the population of the 4f shell rather than by photoemission.

Bremsstrahlung isochromat spectroscopy (BIS or IP : inverse photoemission) is the most direct technique for probing empty states [26]. A beam of electrons (~ 1500 eV) impinging on the sample populates the corresponding high-lying levels. Their strong interaction with the potential in the solid induces radiative processes to empty states above E_F. In BIS, the intensity of the resulting X-ray emission is recorded at a fixed energy so that it corresponds to a well-defined final state which can be varied simply by sweeping the beam energy. XPS and BIS intensities can be inter-

preted within the same framework since they correspond to perfectly symmetrical processes. The right panel of fig. 2 shows the BIS spectra of γ-Ce, $CePd_3$ [17] and $CeRu_2$. For all pure rare earths metals these types of spectra have been succesfully analyzed with the intensities predicted by the fractional parentage coefficients [27,28]. In particular, the main structures above 3 eV in the spectrum of γ-Ce can be unambiguously attributed to the discrete $4f^2$ final states and can be used as a safe fingerprint revealing the $4f^1$ initial configuration of the Ce atoms. The intensity just above E_F is anomalously large compared with that of La [28]. It is possibly due to a small contribution originating from tetravalent Ce atoms at the surface. At least two of the three structures observed in the BIS spectrum of the mixed valent $CePd_3$ are easily interpreted : The $4f^2$ final states are observed at energies larger than 3.5 eV and are slightly shifted away from E_F when compared with those of γ-Ce, the two $4f^1$ final states $^2F_{3/2}$ and $^2F_{7/2}$ appear as a single peak which is pinned at E_F as expected in a mixed valent compound. The middle peak, previously ascribed tentatively to a surface chemical shift [17] is more likely to be attributed to empty d band states. The simplicity of the BIS spectrum of $CeRu_2$ is striking. It contains a main peak showing the featureless shape of the $4f^1$ final states which cannot be confused with the characteristic shape of $4f^2$ final states. The fact that this peak is located a few tenths of an eV higher than in $CePd_3$ suggests that the initial configuration of the Ce ions in $CeRu_2$ is nearly pure $4f^0$. This conclusion is supported by the apparent absence of $4f^2$ final states around 5 eV. Although a weak bump is observed in the $4f^2$ region of the spectrum, its intensity has been found to correlate with the O 1s intensity.

Therefore, we attribute this weak signal to residual contamination, probably Ce_2O_3, which could never be completely eliminated. In our opinion, the BIS spectrum provides strong evidence for the tetravalence of Ce in $CeRu_2$. The BIS process is by far simpler than the transitions involved in any core level spectroscopy. The resulting final state perturbation is much weaker and would not be suspected to induce a large contribution attributable to final states other than those corresponding simply to the single occupation of the levels vacant in the ground state. The contrast between the conclusion which can be drawn from BIS and XPS core level spectra is striking and puzzling. We believe that the assingment of the different states of a Ce atom containing a deep hole or the probability to observe these states in core level spectroscopies urgently need to be re-examined critically. Furthermore, the theoretical models proposes to explain these apparently contradictory results will have to be used to predict BIS spectra. Resonant photoemission has been claimed quite often to be a suitable tool for studying the occupation of the 4f shell in Ce. Considering the impossibility of finding any conclusive difference between the 3d spectra of $CePd_3$ and $CeRu_2$ (fig. 1), in spite of their very dissimilar BIS spectra (fig. 2), we believe that resonant photoemission spectra of Ce compounds [14] might be affected by a similar ambiguity requiring a more circumspect interpretation.

References

[1] J.M. Lawrence, P.S. Riseborough and R.D. Parks, Rep. Prog. Phys. 44 (1981) 1.

[2] L.M. Falicov, W. Hanke and M.B. Maple, eds., Valence fluctuations in solids (North-Holland, Amsterdam, 1981).

[3] P. Wachter and H. Boppart, eds., Valence instabilities (North-Holland, Amsterdam, 1982).

[4] T.F. Smith and I.R. Harris, J. Phys. Chem. Solids 28 (1967) 1846.

[5] H.J. van Daal and K.H.J. Buschow, Phys. Stat. Sol. (b) 3 (1979) 221.

[6] B. Johansson, in: Valence instabilities and related narrow band phenomena, ed. R.D. Parks (Plenum, New York, 1977) p. 435.

[7] S.H. Devare, H.G. Devare and H. de Waard, in: Valence instabilities, eds. P. Wachter and H. Boppart (North-Holland, Amsterdam, 1982) p. 337.

[8] T.F. Smith, H.L. Luo, M.B. Maple and I.R. Harris, J. Phys. F1 (1971) 896.

[9] F.R. De Boer, W.H. Dijkman, W.C.M. Mattens and A.R. Miedema, J. Less-Common Met. 64 (1979) 241.

[10] K.R. Bauchspiess, W. Boksch, E. Holland-Moritz, H. Launois, R. Pott and D. Wohlleben, in: Valence fluctations in solids, eds. L.M. Falicov, W. Hank and M.B. Maple (North-Holland, Amsterdam, 1981) p. 417.

[11] G. Krill, J.P. Kappler, A. Meyer, L. Abadli and M.F. Ravet, J. Phys. F11 (1981) 1713,

[12] P.R. Sarode, D.D. Sarma, C.N.R. Rao, E.V. Sampathkumaran, L.C. Gupta and R. Vijayaraghavan, Mat. Res. Bull. 16 (1981) 175.

[13] P.R. Sarode, D.D. Sarma, R. Vijayaraghavan, S.K. Malik and C.N.R. Rao, J. Phys. C15 (1982) 6655.

[14] J.W. Allen, S.-J. Oh, I. Lindau, M.B. Maple, J.F. Suassuna and S.B. Hagström, Phys. Rev. B26 (1982) 445.

[15] Y. Baer, G. Bush and P. Cohn, Rev. Sci. Instrum. 46 (1975) 446.

[16] J.K. Lang and Y. Baer, Rev. Sci. Instrum. 50 (1979) 221.
[17] Y. Baer, H.R. Ott, J.C. Fuggle and L.E. De Long, Phys. Rev. B24 (1981) 5384.
[18] J.F. Herbst and J.W. Wilkins, Phys. Rev. Lett. 43 (1979) 1760.
[19] J.C. Fuggle, F.U. Hillebrecht, Z. Zolnierek, Ch. Freiburg and M. Campagna, in: Valence instabilities, eds. P. Wachter and H. Boppart (North-Holland, Amsterdam, 1982) p. 267.
[20] S.-J. Oh and S. Doniach, Phys. Rev. B26 (1982) 2085.
[21] O. Gunnarsson and K. Schönhammer, Phys. Rev. Lett. 50 (1983) 604.
[22] G. Thorton and M.J. Dempsey, Chem. Phys. Lett. 77 (1981) 409.
[23] P. Wachter, in: Valence instabilities, eds. P. Wachter and H. Boppart (North-Holland, Amsterdam, 1982) p. 145.
[24] H.R. Moser, E. Wuilloud and Y. Baer, to be published.
[25] G. Krill, L. Abadli, M.F. Ravet, J.P. Kappler and A. Meyer, J. de Phys. 41 (1980) 1121.
[26] Y. Baer, in: Emission and scattering techniques, ed. P. Day (Reidel, Dordrecht, 1981) p.153.
[27] P.A. Cox, J.K. Lang and Y. Baer, J. Phys. F11 (1981) 113.
[28] J.K. Lang, Y. Baer and P.A. Cox, J. Phys. F11 (1981) 121.

PHYSICAL REVIEW B VOLUME 28, NUMBER 12 15 DECEMBER 1983

Rapid Communications

The Rapid Communications section is intended for the accelerated publication of important new results. Manuscripts submitted to this section are given priority in handling in the editorial office and in production. A Rapid Communication may be no longer than 3½ printed pages and must be accompanied by an abstract. Page proofs are sent to authors, but, because of the rapid publication schedule, publication is not delayed for receipt of corrections unless requested by the author.

Electronic structure of γ- and α-Ce

E. Wuilloud, H. R. Moser, W.-D. Schneider, and Y. Baer
Institut de Physique, Université de Neuchâtel, CH-2000 Neuchâtel, Switzerland
(Received 29 August 1983)

The γ-α phase transition in cerium metal has been studied by temperature-dependent bremsstrahlung isochromat, core-level x-ray photoemission, and electron-energy-loss spectroscopy. The experimental results can be coherently analyzed within the many-body formalism of Gunnarsson and Schönhammer. We find that the f occupation n_f is reduced by -15% while the f conduction-electron hybridization Δ increases from $\Delta=25$ meV to $\Delta=60$ meV upon the γ-α phase transition. Thus the change in the coupling Δ is concluded to be the driving mechanism for the γ-α phase transition in Ce metal.

The γ-α phase transition of metallic cerium has been a puzzling subject for a great number of experimental and theoretical efforts.[1-3] Answering the fundamental questions of $4f$ occupancy, $4f$ hybridization width, and $4f$ energy position in the metal has been tried from a variety of different experimental observations (thermochemical data, spectroscopic results, atomic volume, magnetism, superconductivity) with the aid of numerous elaborate theoretical models, but so far no consensus has emerged. For instance, Mårtensson, Reihl, and Parks[4] were able to rule out the promotional model for the γ-α phase transition on the basis of their valence-band photoemission data on $Ce_{0.9}Th_{0.1}$. However, their experiments did not allow explanation of the nature of the phase transition. Later on, Wieliczka, Weaver, Lynch, and Olson[5] explained observed features in their photoemission spectra by increased hybridization of the $4f$ wave function upon entering the α phase. But, as has already been admitted by the authors of Ref. 4, the spectroscopic results clearly establish the need for theoretical focus on the nature of the excited states resulting from photoemission and other spectroscopies. Recently, after a first step by Oh and Doniach,[6] such a theory was presented by Gunnarsson and Schönhammer (GS).[7] Using a slightly modified version of the Anderson impurity Hamiltonian and taking into account the degeneracy N_f of the f level (which was not considered by the authors of Ref. 6) GS center their discussion on the population n_f of the f level and its coupling Δ to the conduction states. Comparison with x-ray absorption spectroscopy (XAS)[8] and x-ray photoemission spectroscopy (XPS)[9] experiments on Ce-metal and a number of Ce intermetallic compounds indicated substantially different values for n_f and Δ than generally assumed. These results shed new light on the possible driving mechanism of the γ-α phase transition in Ce and therefore initiated a new spectroscopic study of this unusual metal employing bremsstrahlung isochromat spectroscopy (BIS), XPS, and electron-energy-loss spectroscopy (EELS).

In this Rapid Communication we present the results of this study for α- and γ-Ce. In particular, different spectral responses are found for the three spectroscopies used, indicating the differences between the realized final states. While the BIS and XPS spectra vary markedly for the two phases, the EELS spectra are nearly identical. We show that these discrepancies can be understood satisfactorily within the GS model. An analysis of our data in terms of this model reveals only small f-count changes (reduction of -15%) but a large increase of the f-hybridization width from 25 to 60 meV upon the γ-α phase transition. Therefore it is argued that the change in f conduction-electron hybridization is mainly responsible for the γ-α phase transition in Ce-metal and not the change in the f occupation. These findings are consistent with previous positron annihilation,[10] Compton scattering,[11] and muon spin rotation measurements.[12]

The samples of γ- and α-Ce were obtained *in situ* by repeated evaporations of Ce onto a polished Cu plate at room temperature and at liquid-nitrogen temperature (80 K), respectively. The pressure did not raise above 1×10^{-10} Torr during the evaporation process. At 80 K the film is essentially composed of α-Ce; the presence of other phases is negligible.[5] The measurements were performed in a combined XPS-BIS-EELS apparatus[13,14] in a vacuum of 1×10^{-11} Torr. Under these conditions, no oxygen contamination could be detected (by monitoring the O 1s region with XPS) during data acquisition (10 h).

The BIS spectra of α- and γ-Ce are shown in Fig. 1. The spectrum of γ-Ce is identical to the one obtained in an earlier work.[15] The main structure, centered between 3 and 7 eV above the Fermi energy, was attributed to transitions to $4f^2$ final-state multiplets, also indicated in Fig. 1 by the bar diagram. Thus, as generally accepted, γ-Ce was considered to be trivalent with an f occupation number $n_f\sim1$ in the initial-state configuration. The spectrum of α-Ce, displayed in the upper part of Fig. 1, differs remarkably from the one of γ-Ce by the narrow line of 0.9 eV full width at half maximum (FWHM) just above the Fermi energy. Under the assumption that this peak corresponds to f^1 final states, split by the spin-orbit interaction, a least-squares analysis was performed with two Gaussian line profiles accounting for experimental resolution and lifetime broadening. The

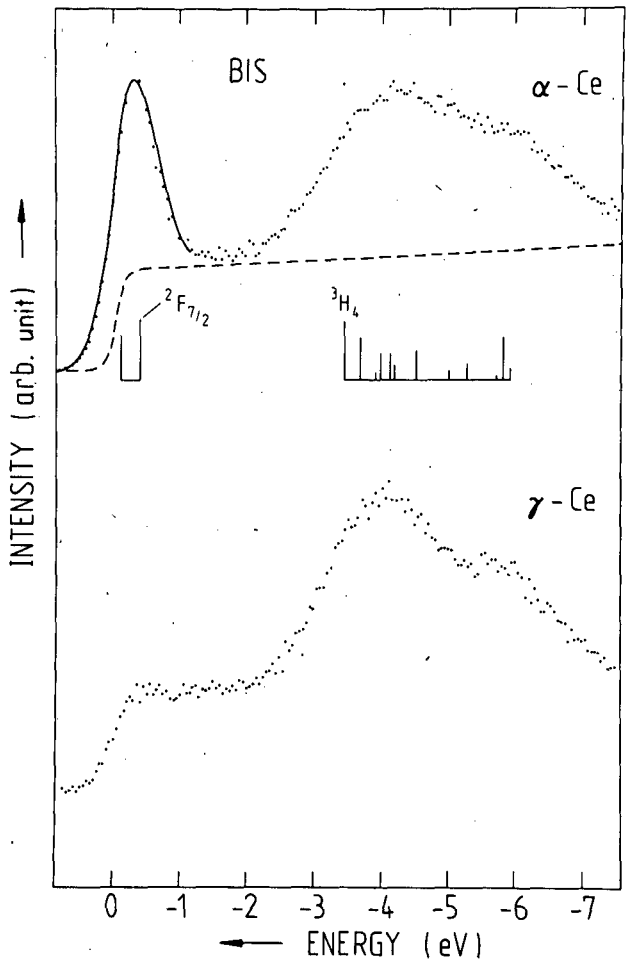

FIG. 1. BIS spectra of γ- and α-Ce. The solid line for α-Ce represents the result of a least-squares analysis of the data points with a $4f^{7/2}$ and $4f^{5/2}$ doublet. Positions and relative intensities are indicated by the bar diagram. The contribution of the underlying *sd* band is indicated by the dashed line (see text). The final-state f^2 multiplet structure was taken from Ref. 16.

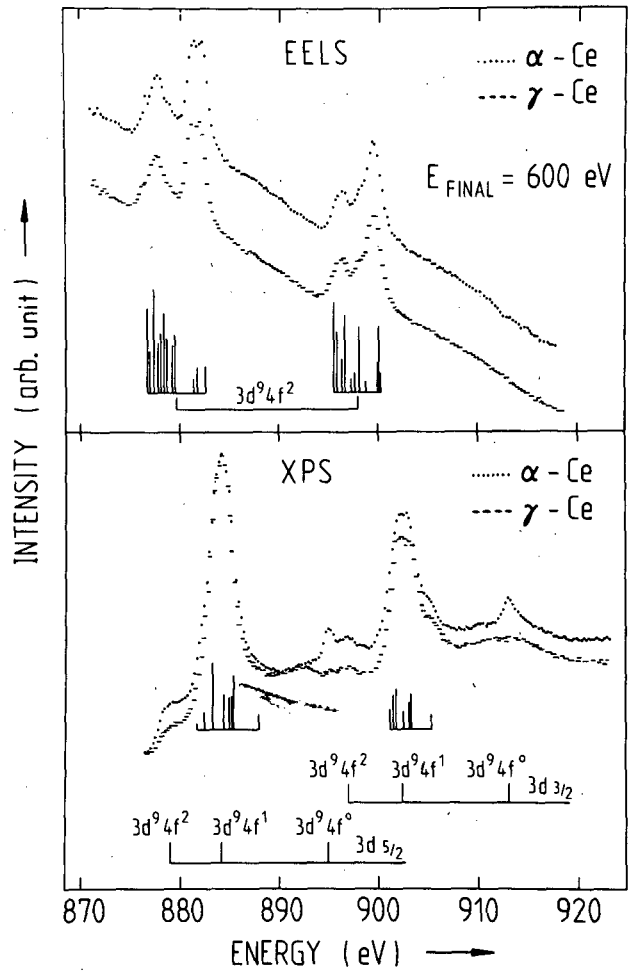

FIG. 2. EELS and XPS $3d$ core-level spectra of γ- and α-Ce on a common energy scale (the elastic peak in EELS is aligned with the Fermi energy of the XPS spectrum). The corresponding final states are indicated. For EELS the $3d^94f^2$ and for XPS the $3d^94f^1$ final-state multiplet structure were taken from Refs. 20 and 17, respectively.

spin-orbit splitting was held fixed at 0.282 eV found for La,[16] while the intensity was varied in the proper ratio $\frac{4}{3}$ of the multiplet components. Furthermore, the contribution of the underlying *sd* conduction-electron states, clearly visible in a BIS-spectrum of La,[16] was simulated by the product of the Fermi function with the density of states in the free-electron model and broadened by a Gaussian, accounting for the finite experimental resolution (dashed line in Fig. 1). The result of this analysis is indicated by the full curve in Fig. I showing good agreement with the data. Thus, we note that (i) the appearance of f^1 and f^2 final-state multiplets in BIS strongly points to the local character of the $4f$ electrons and (ii) the dramatic change in the spectra upon the γ-α phase transition indicates a phase-dependent change of the electronic structure of Ce-metal.

In Fig. 2 the $3d$ core-level XPS and EELS spectra for γ- and α-Ce are displayed on a common energy scale. The structure in the XPS spectra has been interpreted in the conventional way,[9] as indicated by the bar diagram in the bottom of Fig. 2. Multiplet effects due to the coupling of the $3d$ hole with the open $4f$ shell are clearly visible in the $3d_{3/2}$ peak and have been tentatively assigned to the underlying multiplet structure of the $3d^94f^1$ configuration.[17] We note the following observations: (i) There is clear evidence of a $3d^94f^0$ component in α-Ce which is not present in γ-Ce; (ii) the intensity of the $3d^94f^2$ final-state component increases considerably upon the phase transition. These findings again indicate a phase-dependent change of the electronic structure of Ce-metal.

In the upper part of Fig. 2 the EELS spectra of the $3d$ core excitation region for γ- and α-Ce are presented. In γ-Ce the observed structures should correspond to the final-state $3d^94f^2$ configuration.[18] Since in EELS, as recently shown for a few rare-earth metals and oxides, non-dipole-allowed transitions occur with increasing intensity towards the excitation threshold,[18,19] EELS-spectra exhibit considerably more structure than those obtained by XAS.[8] An attempt to compare the spectra with an intermediate coupling calculation of Spector *et al.*[20] yields fair agreement for the energy separation but not for the intensities of the multiplet. This is not surprising, however, in view of the different transition probabilities encountered in EELS, XAS, and XPS. We want to point out that the threshold energy for the $3d$ excitation, i.e., for the occupation of the $3d^94f^2$ final state in EELS, corresponds well to the low-binding-energy rise in the XPS spectrum, giving confirmation of the $3d^94f^2$

assignment. No marked difference is observed for the EELS spectrum of α-Ce, also shown in Fig. 2. If there were an initial-state f^0 contribution, one should observe (similarly to the XAS results on a number of Ce-intermetallics[8]) the corresponding $3d^94f^1$ final-state contributions around 805 and 905 eV. A close inspection of this spectral region reveals a slightly larger drop of the background intensity in α-Ce than in γ-Ce at 891 and 911 eV, respectively. This might indicate the presence of the $3d^94f^1$ configuration in α-Ce.

To summarize the experimental situation we note the following: Each type of spectroscopy yields a different picture of the electronic states in γ- and α-Ce. In order to formulate this observation more quantitatively, we have evaluated the following intensity ratios,[21] which should be directly related to the f occupation in the initial state: $f^1/(f^1+f^2)$ from BIS and $f^0/(f^0+f^1+f^2)$ from XPS. The results are listed in columns 1 and 2 of Table I. For α-Ce BIS indicates an f occupation $n_f\sim 0.78$, XPS gives $n_f\sim 0.95$, and EELS (not shown in the table) yields $n_f\sim 1$. These discrepancies show immediately that the final-state f occupation is a different function of the initial-state occupancy for each type of spectroscopy. This fact must be attributed to the different degree of perturbation which the electronic system undergoes by interaction with electrons or photons. In XPS we are left with a core-hole state, in BIS with an additional f electron, and in EELS with both a core-hole plus an electron in the valence states. Oh and Doniach[6] were the first to consider such a problem for Ce systems. However, they did not treat the degeneracy of N_f of the f level in their model. Recently, GS, by including the degeneracy, took a decisive step forward in the understanding of the response of Ce-systems to an experimental probe. They were able to show how to trace back final-state to initial-state properties. In particular, they calculated BIS, XPS, and XAS spectra and discussed how experimental spectra can be used to estimate the f occupancy n_f and the coupling Δ between the f level and the conduction states. Comparison of the theory with XAS (Ref. 8) and XPS (Ref. 9) spectra on a number of Ce compounds was very successful. In general, f occupancies $n_f>0.7$ and hybridization widths of the order of $\Delta\sim 0.1$ eV were obtained. The question arises whether this formalism is also applicable to the γ-α phase transition in Ce-metal and if the parameters deduced can give insight into the driving mechanism of the phase transition.

In order to derive the coupling Δ from the experimentally determined intensity ratios $f^2/(f^1+f^2)$ in XPS (Ref. 9) we use Figs. 5 and 6 of Ref. 9 where the dependence of this ratio on n_f and Δ is given. For γ- and α-Ce we obtain $\Delta=25\pm 5$ meV and $\Delta=60\pm 10$ meV, respectively. The errors are due to uncertainties in the intensity ratios[21] and to the approximations in the theory.[7,9] For γ-Ce good agreement with an earlier derivation is obtained.[9] In order to determine the ground-state f occupation from XPS we use Fig. 4 of Ref. 9, where the dependence of the ratio $f^0/(f^0+f^1+f^2)$ on the initial f occupation is given explicitly for $\Delta=60$ meV. The analysis of the BIS intensity ratios $f^1/(f^1+f^2)$ is performed with the aid of Figs. 11 and 7 of Ref. 7, where the dependence of this quantity on the ground-state f occupation for $\Delta=80$ meV and $\Delta=120$ meV are calculated, respectively. The results for Δ and n_f are summarized in Table I. As a matter of fact, within this theory, consistent values for n_f are obtained in both spectroscopies. This gives confidence in the reliability of the theory. The question of why there are only small changes in the EELS spectra of γ- and α-Ce still remains to be answered. So far GS included in their theory the discussion of BIS, XPS, and XAS spectra. However, it is possible, as we shall show, to extend qualitatively their arguments to the EELS case: According to GS the deviation from linearity of the intensity ratios in the final-state versus the ground-state f-occupation number depends on the coupling between the f^0 and f^1 configuration in the initial state ($N_f\Delta\sim 2$ eV) relative to the energy separation between these states in the final state. If this energy separation is large compared to 2 eV as encountered in XPS (11 eV) the f^0 weight in the final state is not much smaller than in the initial state. With decreasing energy separation in the final state the f^0 weight in the final state should decrease. Thus, in XAS (now the final f^1 and f^2 configurations are taken into consideration), this energy separation is only ~ 5 eV and therefore the f^1 final state in XAS should loose considerable weight as compared to the f^0 final state in XPS. In fact, this behavior has been observed for Ce compounds.[8,9] Now, in EELS, the presence of nondipole allowed transitions closes even more the energy gap between the final f^1 and f^2 states, thus leading to a pronounced weight loss of the f^1 final state in the spectra. In this way the very small f^1 contribution in the EELS spectra of α-Ce can be understood.

Evidently, the GS model seems to be able to describe consistently the observed spectra obtained in BIS, XPS, and EELS. Therefore we go back to Table I and summarize the essential result of this investigation: While the f-occupation number n_f is only slightly reduced ($\sim 15\%$) the hybridization Δ is increased by more than a factor of 2 (from $\Delta=25$ to $\Delta=60$ meV) upon the γ-α phase transition in Ce-metal.

TABLE I. Peak intensity ratios for α- and γ-Ce as determined by BIS and XPS core-level spectroscopy. We stress that due to the superposition of $3d^94f^2$ and $3d^94f^1$ multiplets the determination of Δ on the basis of XPS $3d$ core level spectra leads only to a lower limit of this value (see Fig. 2). The values for the f-occupation n_f and the $4f$ conduction-electron hybridization Δ were derived on the basis of the Gunnarsson-Schönhammer model (Ref. 7).

	$\frac{f^1}{f^1+f^2}$ (BIS)	$\frac{f^0}{f^0+f^1+f^2}$ (XPS)	$\frac{f^2}{f^1+f^2}$ (XPS)	Δ (meV)	$n_{f_{\mathrm{XPS}}}$	$n_{f_{\mathrm{BIS}}}$
γ-Ce	<0.01	<0.01	0.05	25	~ 1	~ 1
α-Ce	0.22	0.05	0.11	60	0.90	0.85

Thus, we conclude that the dominant driving mechanism of the phase transition is given by the change in the coupling Δ rather than by the change in the f occupancy.

The consequences of this finding imply that the increase in f-conduction electron hybridization is also responsible for the loss of magnetism in α-Ce.[7] Furthermore, through the increase of Δ the $4f$ electrons are able to participate in the bonding, thereby directly influencing the lattice constant in a nonlinear way.[7,9,22] Of course, there still remain problems to be solved. Among others, why is the γ-α phase transition in Ce-metal of the first-order type?

ACKNOWLEDGMENTS

The authors wish to thank O. Gunnarsson for stimulating discussions. This work is supported by the Swiss National Science Foundation.

[1] J. M. Lawrence, P. S. Riseborough, and R. D. Parks, Rep. Prog. Phys. 44, 1 (1981).

[2] *Valence Fluctuations in Solids,* edited by L. M. Falicov, W. Hanke, and M. B. Maple (North-Holland, Amsterdam, 1981).

[3] *Valence Instabilities,* edited by P. Wachter and H. Boppart (North-Holland, Amsterdam, 1982).

[4] N. Martensson, B. Reihl, and R. D. Parks, Solid State Commun. 41, 573 (1982).

[5] D. Wieliczka, J. H. Weaver, D. W. Lynch, and C. G. Olson, Phys. Rev. B 26, 7056 (1982).

[6] S. J. Oh and S. Doniach, Phys. Rev. B 26, 2085 (1982).

[7] O. Gunnarsson and K. Schönhammer, Phys. Rev. Lett. 50, 604 (1983); (unpublished).

[8] J. C. Fuggle, F. U. Hillebrecht, J.-M. Esteva, R. C. Karnatak, O. Gunnarsson, and K. Schönhammer, Phys. Rev. B 27, 4637 (1983).

[9] J. C. Fuggle, F. U. Hillebrecht, Z. Zolnierek, R. Lässer, Ch. Freiburg, O. Gunnarsson, and K. Schönhammer, Phys. Rev. B 27, 7330 (1983).

[10] D. R. Gustafson, J. D. McNutt, and L. D. Roelling, Phys. Rev. 183, 435 (1969); R. F. Gempel, D. R. Gustafson, and J. D. Willenberg, Phys. Rev. B 5, 2082 (1972).

[11] J. Felsteiner, M. Heipler, and D.-F. Berggren, Solid State Commun. 32, 343 (1979); V. Kornstädt, R. Lässer, and B. Lengeler, Phys. Rev. B 21, 1898 (1980).

[12] H. Wehr, K. Knorr, F. N. Gygax, A. Schlenck, and W. Studer, Phys. Rev. B 24, 4041 (1981).

[13] J. K. Lang and Y. Baer, Rev. Sci. Instrum. 50, 221 (1979).

[14] H. R. Moser, Ph.D. thesis No. 7369, Eidgenoessische Technische Hochschule, Zurich, 1983 (unpublished).

[15] Y. Baer, H. R. Ott, J. C. Fuggle, L. E. De Long, Phys. Rev. B 24, 5384 (1981).

[16] J. K. Lang, Y. Baer, and P. A. Cox, J. Phys. F 11, 121 (1981).

[17] J.-M. Esteva, R. C. Karnatak, J. C. Fuggle, and G. A. Sawatzky, Phys. Rev. Lett. 50, 910 (1983).

[18] J. A. D. Matthew, G. Strasser, and F. P. Netzer, Phys. Rev. B 27, 5839 (1983).

[19] F. P. Netzer, G. Strasser, and J. A. D. Matthew, Phys. Rev. Lett. 51, 211 (1983).

[20] N. Spector, C. Bonelle, G. Dufour, C. K. Jørgensen, and H. Berthov, Chem. Phys. Lett. 41, 199 (1976).

[21] The experimentally determined numbers have an accuracy of about 10% which can be attributed to the uncertainty of the decomposition of the spectra.

[22] G. Neumann, R. Pott, J. Röhler, W. Schlabitz, D. Wohlleben, and H. Zahel, in *Valence Instabilities,* edited by P. Wachter and H. Boppart (North-Holland, Amsterdam, 1982), p. 87.

PHYSICAL REVIEW B VOLUME 29, NUMBER 9 1 MAY 1984

High-energy spectroscopic study of the electronic structure of UBe_{13}

E. Wuilloud and Y. Baer
Institut de Physique, Université de Neuchâtel, Rue A.-L. Breguet 1, CH-2000 Neuchâtel, Switzerland

H. R. Ott
Laboratorium für Festkörperphysik, Eidgenössische Technische Hochschule–Hönggerberg, CH-8093 Zurich, Switzerland

Z. Fisk and J. L. Smith
Los Alamos National Laboratory, Los Alamos, New Mexico 87545

(Received 7 February 1984)

X-ray photoemission and bremsstrahlung isochromat spectroscopies have been used to probe the occupied and unoccupied states of UBe_{13}. Between two and three electrons are found to populate the tail of a surprisingly broad $5f$ band (~ 5 eV) of extended states. With our resolution ($\lesssim 0.5$ eV) it is not possible to observe directly at the Fermi energy any peculiarity of the density of states explaining the extraordinary properties of this compound. However, the drastic differences between the core-level spectra of U and Be indicate that the $5f$ states remain essentially confined around the U atoms and are only weakly hybridized with the sp-band states originating from the Be atoms.

The recent discovery of bulk superconductivity in UBe_{13} below 1 K (Ref. 1) has given clear evidence for the existence of strongly interacting electrons in some metallic materials, giving rise to anomalous properties at low temperatures. Other examples for this type of materials are $CeAl_3$ (Ref. 2) and $CeCu_2Si_2$ (Ref. 3), again two compounds containing f electrons, obviously a prerequisite for the observation of the behavior to be discussed here. All these compounds show an anomalously large specific heat $c_p(T)$ at low temperatures. In $CeAl_3$, $c_p(T)$ decreases linearly with decreasing temperature below 1 K but, in comparison with normal metals, with a very large coefficient γ of the order of 1.5 J/mole K^2,[2] indicating a considerable renormalization of the electronic subsystem. In UBe_{13} (Ref. 1) and $CeCu_2Si_2$,[3] this linear decrease with a slope of about 1 J/mole K^2 is intercepted by a discontinuity Δc due to a superconducting transition. In both cases, the magnitude of Δc is compatible with the large values of c_p/T just above the transitions and the experimental verification that the entropy difference between the superconducting and the normal state is zero below T_c demonstrates that it is indeed the strongly interacting electrons that are involved in the superconducting state.

These high γ values are necessarily also based on large densities of electronic states at the Fermi energy E_F, implying very narrow features in the energy dependence of the electronic structure at E_F. The possible occurrence of such features is well known from theoretical work concerning the electronic structure of simple metals containing transition-metal impurities in the dilute limit.[4] Recent work considering concentrated systems[5] claims that similar narrow resonances at E_F also appear in this case. Information on the energy dependence of the electronic structure of a metal is provided by using photoemission techniques. A first attempt concerning UBe_{13} involved resonant photoemission, favoring the emission of electrons with f symmetry, by scanning the energy range below E_F to about 12-eV binding energy.[6] Since also core-electron spectra and particularly the energy distribution of empty electron states provide valuable information, we chose to map parts of the electronic spectrum of UBe_{13} by using x-ray photoemission (XPS) and bremsstrahlung-isochromat spectroscopy (BIS).

The sample investigated in the present study was a platelet cut from the same polycrystalline batch of material that was used for previous specific-heat measurements.[7] The XPS and BIS spectra were obtained in a combined instrument described elsewhere.[8,9] The contamination was removed from the sample surface by scraping it *in situ* with an Al_2O_3 file until the O $1s$ and C $1s$ XPS signals could no longer be detected in a 5-min scan. The base pressure of 1×10^{-11} Torr in the instrument allowed us to accumulate the different spectra during periods of many hours without any sizable degradation of the surface cleanliness.

The occupied valence-band states of UBe_{13} have recently been studied by resonant photoemission.[6] The spectra have been interpreted as revealing a UBe_{13} density of states (DOS) looking rather like a superposition of the DOS of the two pure constituents U and Be. A calibration procedure of the intensity of the different signals in the spectra has yielded a $5f$ population of roughly one electron. Our XPS valence band spectrum of UBe_{13} is shown on the left side of Fig. 1. In the energy range from the Fermi energy E_F to -4 eV it is in good agreement with the previously published spectrum excited at 40 eV.[6] The sp states of Be forming a broad band[10] have a very weak cross section at the Al $K\alpha$ photon energy. From atomic cross-section calculations[11] they are estimated to represent less than 10% of the total intensity of the XPS spectrum and for this reason they do not emerge from the background of inelastically scattered electrons extending at higher binding energies. In U, the atomic cross section for the $5f$ states is substantially larger than the one for the $6d$ states $[\sigma(5f^1)/\sigma(6d^1)=6]$ (Ref. 11) and the XPS peak must be mainly attributed to the tail of the $5f$ band cut by E_F. This spectrum of UBe_{13} shows a striking similarity with the spectrum of α-U metal[12] despite the different environment of the U atoms and their

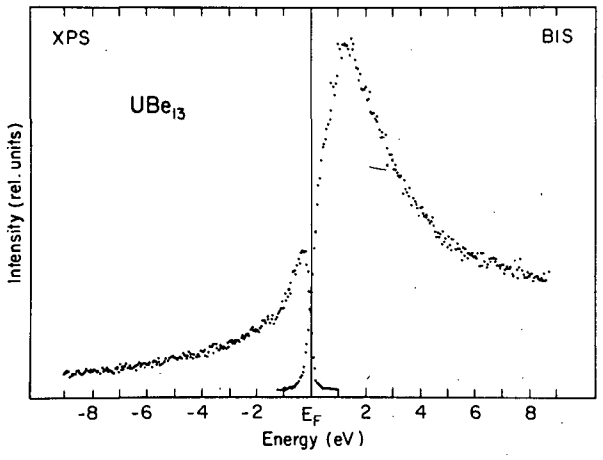

FIG. 1. Combined XPS–BIS spectrum of UBe_{13}. The relative intensities below and above E_F have been scaled by a continuity criterion (see text).

separation which is more than 50% larger in UBe_{13} than in α-U.

In a limited energy range above E_F the unoccupied states have been probed by BIS and the corresponding spectrum is shown on the right side of Fig. 1. Since the matrix elements for the BIS transitions are practically the same as those accounting for XPS transitions, also the BIS spectrum represents nearly exclusively the empty $5f$ states superimposed on a background increasing toward higher energies and attributable to electrons which have been scattered inelastically prior to the BIS process. Whereas two marked peaks are observed in α-U,[12] the BIS spectrum of UBe_{13} shows a single and featureless peak with its maximum at 1.3 eV. On the low-energy side, the clear change of slope at 0.4 eV allows us to observe the position of the Fermi edge which is found to coincide with the position determined by the usual energy-scale calibration performed with Au. The Koopmans's approximation is very accurate at the Fermi energy of metals,[13] so that it is well justified to join the XPS and BIS spectra at E_F in order to depict the whole $5f$ band. The main uncertainty in this attempt is the calibration of the relative intensities observed with the two different techniques. In the present situation, the comparison of the Fermi-edge intensities is not suitable: the two techniques have different line shapes and linewidths[8,9] and, furthermore, E_F is located in a very steep DOS. A more reliable approach in determining the relative intensities consists in joining the two spectra above and below the range affected by the Fermi cutoff by a smooth curve. As shown in Fig. 1, this criterion allows us to represent rather precisely a continuous DOS crossing E_F. After subtraction in both spectra of a background proportional to the integrated signal intensity from E_F to the respective energy and joining smoothly the spectra away from E_F, the area of the two curves represent the total band intensity.

As mentioned previously, the contribution of the $l=2$ projected DOS to the spectra is small but not entirely negligible. For this reason the experimental intensity ratio $I_{BIS}/I_{XPS}=3.7$ does not directly represent the ratio of the empty to occupied $5f$ states but it must be corrected for the presence of the ten $6d$ states located in the same energy range. It is straightforward to express I_{BIS}/I_{XPS} as a function of the numbers of the occupied states (n_f, n_d) and of the cross-section ratio $\sigma(5f^1)/\sigma(6d^1)=6$ (Ref. 11):

$$\frac{I_{BIS}}{I_{XPS}}=\frac{(10-n_d)+(14-n_f)\sigma_f/\sigma_d}{n_d+n_f\sigma_f/\sigma_d} \quad . \tag{1}$$

In a metallic bond, only a very small charge transfer is expected between the Be and U atoms, as confirmed below in the discussion of the core level binding energies. The approximate neutrality around the U atoms yields the additional condition for the number of occupied f and d states $n_d+n_f\cong 6$ which allows us to extract the value $n_f\cong 2.8$. The uncertainties affecting the numbers used in this estimation are not influencing markedly the value found for n_f. In order to demonstrate this fact, we have calculated the range of each parameter for which n_f varies from 2 to 3:

$$3.5\leq I_{BIS}/I_{XPS}\leq 4.9 \ ;$$

$$1.75\leq \sigma(5f^1)/\sigma(6d^1)\leq 19 \ ;$$

$$5.4\leq n_d+n_f\leq 10.4 \ .$$

The variation of (n_d+n_f) describes implicitly the neglected presence in U of s and p states which have different cross sections than the d states. The acceptable errors in these numbers are smaller than these limits and we can safely conclude that the metallic band of UBe_{13} is occupied by a number of $5f$ electrons not far from 3, but in any case between 2 and 3. This result is in disagreement with the value of $n_f\cong 1$ derived from previous photoemission spectra excited by low-energy photons.[6] Less surprising is the discrepancy with the value of n_f between 1 and 2 predicted by a free-ion interpretation of the effective paramagnetic moment of $3.08\mu_B$.[7]

Figure 2 shows the XPS spectrum of the $5f$ core level of U. The maximum of the $4f_{7/2}$ line located at 377.35 eV can be considered to yield accurately the binding energy of this level. It lies in the narrow energy range from 377.1 to 377.4 eV where the $4f_{7/2}$ binding energies of α-U, US, UAs, USb are found.[14] It is interesting to note that the peculiar behavior of UTe manifests itself by a binding energy of 378.1 eV (Ref. 14) and the tetravalence of the U ions containing two $5f$ localized electrons in UPd_3 (Ref. 15) and UO_2 (Ref. 16) by the still higher values of 379.0 and 380.25

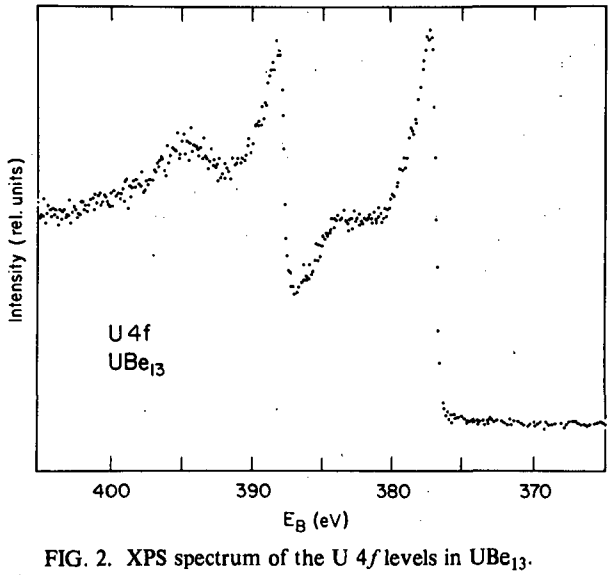

FIG. 2. XPS spectrum of the U $4f$ levels in UBe_{13}.

eV, respectively. These observations confirm our intensity analysis of the outer level spectra leading to the conclusion that the $5f$ population is undoubtedly larger than 2. The very pronounced asymmetrical shape of the lines shown in Fig. 2 reflects a high metallic DOS around E_F allowing the excitation of a great number of low-energy electron-hole pairs in the screening mechanism of the core hole around the U ions.

An intense and broad satellite is also observed at about a 7 eV larger binding energy than each main $4f$ signal. The satellites most likely account for an atomiclike reaction of the outer electrons to the deep hole creation and are due to a local breakdown of the band behavior around the ionized atom. Such effects are particularly intense in narrow bands where the correlation is so important that the large relaxation energy requires the existence of such highly excited final states. The exact nature of this puzzling final state is not established but it may correspond to an integral $5f$ occupation ($5f^2$ or $5f^3$). It has been pointed out[17] that the intensity of this satellite observed in many different U compounds is to some extent correlated with the value of the effective paramagnetic moment, a fact which is also verified in UBe_{13}. Probably the hybridization strength of the $5f$ states of U with the *sp* orbitals of the numerous surrounding Be atoms is the key parameter of this problem and not the U-U spacing.[17,18] In UBe_{13} this hybridization seems to be just strong enough to involve the $5f$ states in the band but can still be locally broken by the atomic potential increase resulting from the core-level ionization. This situation could provide an explanation for the correlation observed between high values of the effective paramagnetic moment and intense satellites.[17] Finally, the absence of shake-down satellite is a further confirmation of the extended nature of the $5f$ states.[14]

So far we have been concerned essentially with the local DOS around the U atoms and originating from $5f$ and $6d$ states. Interesting information on the Be valence states can be obtained indirectly from the Be $1s$ spectrum shown in Fig. 3. The binding energy of 111.2 eV is identical to that found in pure Be metal,[10] at least within the uncertainty associated with the absolute energy calibration. Compared to the drastic asymmetry of the U $4f$ lines shown in Fig. 2, this narrow line [observed full width at half maximum (FWHM) = 0.70 eV] contains obviously only a moderate amount of electron-hole pairs. As expected, the satellite associated with the localized U final state is not excited in the Be $1s$ ionization process. The spectrum of Fig. 3 confirms[6] that around the Be atoms the local DOS is very little disturbed by the presence of the U atoms. This observation is not surprising in view of the high dilution of the U atoms in the Be matrix.

The essential feature of the UBe_{13} electronic structure emerging from this study is that the $5f$ states of U can only get a delocalized character by a weak hybridization with the *sp* wave function tails of the four Be atoms located on the cube faces midway between two nearest U atoms which are too far apart to form a band by direct f-f overlap.[19] The densities of states deriving from U and Be atoms remain rather well separated in space as demonstrated by the dramatically different line shapes observed for the core-level

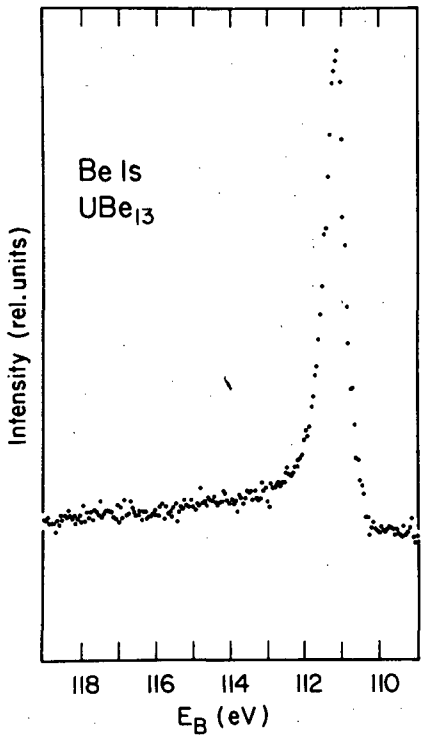

FIG. 3. XPS spectrum of the Be $1s$ level in UBe_{13}.

excitations of the two different kinds of atoms. The outer level spectra presented here reflect nearly exclusively the U states which are obviously responsible for the unconventional properties of UBe_{13}. The limited resolutions of XPS (0.3 eV) and BIS (0.5 eV) allow us to obtain only an overall picture of the DOS which cannot provide any evidence for the mechanism driving the transition from a paramagnetic regime to a superconducting state or for the origin of the enormous low-temperature electronic specific heat. With decreasing temperature one might anticipate a further weakening of the coupling between *sp* and *f* states resulting in an increase of the correlation and effective mass of the $5f$ states. This situation can be thought to favor a ground state dominated by an interaction of magnetic origin.[7] In view of the unexpected broad XPS–BIS $5f$ spectrum recorded at room temperature, it seems illusory to develop models where the total $5f$ bandwidth is supposed to be of the order of 1 meV to explain the exciting low-temperature properties of UBe_{13}. Only the electrons in the immediate vicinity of E_F can be expected to display an extraordinary behavior. Spectroscopic measurements with higher resolution and at low temperature should help to elucidate the mechanisms responsible for this puzzling problem.

We (E.W. and Y.B.) acknowledge fruitful discussions with W.-D. Schneider. In Switzerland, this work was supported by the Schweizerische Nationalfonds zur Förderung der Wissenschaftliche Forschung and, in the U.S.A., was performed under the auspices of the U.S. Department of Energy.

[1]H. R. Ott, H. Rudigier, Z. Fisk, and J. L. Smith, Phys. Rev. Lett. 50, 1595 (1983).
[2]K. Andres, J. E. Graebner, and H. R. Ott, Phys. Rev. Lett. 27, 1779 (1975).
[3]F. Steglich, J. Aarts, C. D. Bredl, W. Lieke, D. Meschede, W. Franz, and H. Schäfer, Phys. Rev. Lett. 43, 1892 (1979).
[4]See, e.g., G. Grüner and A. Zawadowski, *Progress in Low Temperature Physics,* edited by D. F. Brewer (North-Holland, Amsterdam, 1978), Vol. VII B, p. 591.
[5]See, e.g., R. M. Martin, Phys. Rev. Lett. 48, 362 (1982).
[6]G. Landgren, Y. Jugnet, J. F. Morar, A. J. Arko, Z. Fisk, J. L. Smith, H. R. Ott, and B. Reihl, Phys. Rev. B 29, 493 (1984).
[7]H. R. Ott, H. Rudigier, Z. Fisk, and J. L. Smith, in *Moment Formation in Solids,* edited by W. J. L. Buyers, proceedings of the NATO Advanced Studies Institute Series B, Physics (Plenum, New York, in press).
[8]Y. Baer, G. Busch, and P. Cohn, Rev. Sci. Instrum. 46, 446 (1975).
[9]J. K. Lang and Y. Baer, Rev. Sci. Instrum. 50, 221 (1979).
[10]H. Höchst, P. Steiner, and P. Hüfner, Z. Phys. B 30, 145 (1978).
[11]J. H. Scofield, J. Electron. Spectrosc. 8, 129 (1976).
[12]Y. Baer and J. K. Lang, Phys. Rev. B 21, 2060 (1980).
[13]J. F. Janak, Phys. Rev. B 18, 7165 (1978).
[14]Y. Baer, in *Handbook of the Physics and Chemistry of the Actinides,* edited by A. J. Freeman and J. Lander (North-Holland, Amsterdam, in press).
[15]Y. Baer and H. R. Ott, Solid State Commun. 36, 387 (1980).
[16]Y. Baer and J. Schoenes, Solid State Commun. 33, 885 (1980).
[17]W.-D. Schneider and C. Laubschat, Phys. Rev. Lett. 46, 1023 (1981).
[18]W.-D. Schneider and C. Laubschat, Phys. Rev. B 25, 997 (1981).
[19]The crystal structure of UBe_{13} is described in N. C. Bänziger and R. E. Rundle, Acta Crystallogr. 2, 258 (1979).

J. Phys. C: Solid State Phys., 17 (1984) 4799–4806. Printed in Great Britain

Boron induced changes in the electronic structure of $CePd_3$

E Wuilloud†, W-D Schneider†, B Delley†, Y Baer† and F Hulliger‡
† Institut de Physique, Université de Neuchâtel, CH-2000 Neuchâtel, Switzerland
‡ Laboratorium für Festkörperphysik, ETH Zürich, CH-8093 Zürich, Switzerland

Received 30 December 1983

Abstract. The intermetallic compound system $CePd_3B_x$, with $x = 0, 0.12, 0.25$ and 0.5, has been studied by x-ray photoemission, Bremsstrahlungsisochromat and electron energy loss spectroscopy. As a function of the boron concentration strong variations of the occupied and unoccupied parts of the valence bands as well as of the 3d core levels are observed. An analysis of the data within the Gunnarsson–Schönhammer (GS) model yields an f occupation varying from $n_f \sim 1$ in $CePd_3B_{0.5}$ to $n_f \sim 0.9$ in $CePd_3$ (90 K), while the f conduction electron hybridisation remains about constant over the entire composition range with $\Delta = 150 \pm 20$ meV. Moreover a non-linear dependence of the lattice contraction on the f occupancy is found which is well accounted for by a calculation performed within the GS model.

1. Introduction

The electronic structure of cerium metal and its intermetallic compounds has been and remains a puzzling problem leaving many fundamental questions without definite answers. Many experiments have been performed and various theoretical models have been proposed in order to elucidate the different parameters commonly used to describe the 4f level, as its 'bare' energy, its occupation and its coupling to the conduction electrons (Lawrence *et al* 1981, Falicov *et al* 1981, Wachter and Boppart 1982). Recently, the γ–α phase transition in cerium metal has been studied by Bremsstrahlungs-Isochromat (BIS), core level x-ray photoemission (XPS) and electron energy loss (EELS) spectroscopy (Wuilloud *et al* 1983). All experimental results could be consistently analysed within the many-body formalism of Gunnarsson and Schönhammer (1983a, b) (referred to as GS). Since the f occupation, n_f, was found to be reduced only by ~15% while the f conduction electron hybridisation Δ increased from ~25 meV to ~60 meV in the γ–α transition, it was concluded that the change in the coupling was the dominant mechanism driving the phase transition. The consequence of this finding implies that through the increase of Δ the 4f electron is able to participate in the bonding and to influence the lattice constants (Gunnarsson and Schönhammer 1983b). In order to test these ideas we have looked for a system where the lattice constant can be varied systematically and the concomitant changes of Δ and n_f can be observed by electron spectroscopies. Such a situation is met in the rare-earth compound $CePd_3$ (Holland-Moritz *et al* 1977, Krill *et al* 1980, Gupta *et al* 1980, Peterman *et al* 1982, Fuggle *et al* 1983b, c) where the addition of boron was found to cause a volume expansion without changing the crystal structure

0022-3719/84/274799 + 08 $02.25

(Dhar *et al* 1981a, b). On the basis of their lattice parameter and susceptibility measurements, Dhar *et al* concluded that addition of boron induces a valence change of Ce from the mixed valent state in $CePd_3$ to an almost trivalent state in $CePd_3B_{0.5}$. However, as pointed out by these authors, the valence change of Ce may represent only one consequence of the presence of boron. It can also contribute electrons to the conduction band which can have a modified structure in these compounds. In order to investigate the electronic structure changes resulting from addition of boron, a combined BIS, XPS and EELS study was carried out on polycrystalline samples of $CePd_3B_x$ with $X = 0, 0.12, 0.25$ and 0.5, corresponding to lattice parameters increasing from $a = 4.122$ Å to $a = 4.203$ Å (Dhar *et al* 1981a). In order to extend the available lattice constant range, $CePd_3$ was also studied at $T = 90$ K, corresponding to $a = 4.108$ Å (Harris and Raynor 1965). The analysis of the spectroscopic results within the GS framework yields the same coupling constant $\Delta = 150 \pm 20$ meV for the whole compound series, and an f occupation change from $n_f \sim 0.9$ in $CePd_3$ ($T = 90$ K) to $n_f \sim 1$ in $CePd_3B_{0.5}$. As a consequence of the large value of Δ this modest population increase can still induce a sizable lattice expansion. Its non-linear dependence on n_f can be well accounted for by a calculation within the GS model. Finally boron-induced hybridisations among the occupied Pd 4d and empty Ce 5d valence band states are observed.

2. Experimental

All samples were prepared by arc melting of stoichiometric amounts of the constituent elements. Powder x-ray diffraction patterns showed that the samples are single-phase compounds with the cubic $AuCu_3$-type structure. The Ce atoms occupy the cube corners while the Pd atoms are centred on the cube faces. The most likely position for the B atom is the octahedral lattice site (Dhar *et al* 1981a). The spectra presented in this study were obtained in a combined XPS–BIS–EELS spectrometer allowing all measurements to be performed in a vacuum of 1×10^{-11} Torr (Lang and Baer 1979, Moser 1983). The samples were scraped *in situ* with an Al_2O_3 file in order to get clean surfaces. The degree of contamination was checked by recording the O 1s and C 1s XPS signals, which in all cases were below the limit of detectability.

3. Results and discussion

3.1. Valence bands

Figure 1 shows the occupied and empty valence bands of the system $CePd_3B_x$ as obtained by XPS and BIS, respectively. The spectra of $CePd_3$ have been reported previously with the following interpretation (Baer *et al* 1981). The main intensity contribution to the occupied valence bands is attributed to the emission from the filled Pd 4d band. Owing to the unfavourable 4f/4d population and cross section ratios, the 4f contribution to the total XPS intensity is only ~2%. Since the isostructural compound $LaPd_3$ shows considerably less intensity near the Fermi energy (Fuggle *et al* 1983b), the emission between E_F and -0.5 eV is ascribed to the emission from occupied 4f states. Correspondingly, the BIS peaks at 0.5 and around 5 eV above the Fermi energy are assigned to the population of localised $4f^1$ and $4f^2$ multiplets. The structure centred around 2.3 eV above E_F was only recently attributed to a narrow Ce 5d resonance (Hillebrecht *et al* 1983, Hüfner *et al* 1983, Laubschat *et al* 1983), which is a typical feature of this class of materials

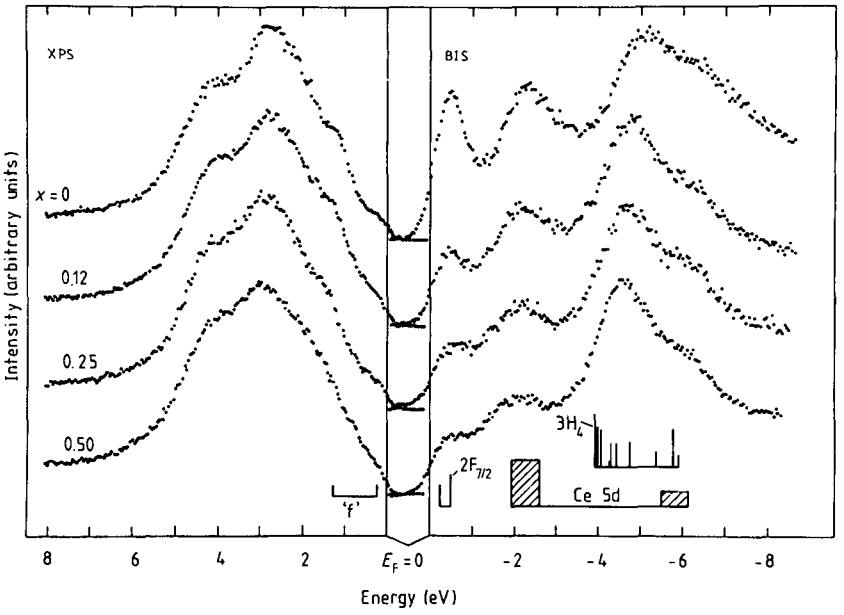

Figure 1. XPS and BIS spectra around E_F of $CePd_3B_x$ for various concentrations x. The relative scaling is arbitrary. The positions of the f emission features are indicated by the bar diagram. The cross-hatched areas represent positions, width and relative intensities of the unoccupied Ce 5d band states for $CePd_3$, and are taken from Laubschat *et al* (1983).

crystallising in the $AuCu_3$ structure (Koenig 1983). The bar diagram in the bottom of figure 1 indicates the expected position and width of the observed spectral features, where the multiplet positions for the $4f^1$ and $4f^2$ states are taken from Wuilloud *et al* (1983) and Lang *et al* (1981), respectively, and the energy positions for the unoccupied Ce 5d states from Laubschat *et al* (1983). Very recently a great attention has been devoted to the Ce 4f excitation in photoemission spectra. In $Ce_{0.9}Th_{0.1}$ (Mårtensson *et al* 1982) and a number of Ce compounds (Allen *et al* 1981, Croft *et al* 1981), resonant photoemission has established the existence of two peaks showing a characteristic 4f behaviour. In $CePd_3$ the structures near E_F and at 1.3 eV are likely to correspond to these 4f excitations. By analogy with the Ni satellite, an attempt has been made to attribute simply these two final states to different screening mechanisms (Hüfner and Steiner 1982a, b). The existence of two '4f' final states in valence band photoemission spectra of Ce and its intermetallic compounds is also predicted by different many-body calculations (Gunnarsson and Schönhammer 1983a, b, Liu and Ho 1982, Fujimori 1983).

The changes of the electronic structure of $CePd_3$ where boron is introduced into this compound is clearly reflected in both the occupied and the empty part of the valence band spectra shown in figure 1. The most striking feature is the decrease of the $4f^1$ emission in the BIS spectra for increasing boron concentration, indicating that Ce in $CePd_3B_{0.5}$ is essentially trivalent as in γ-Ce (Baer *et al* 1981). Intuitively one expects a corresponding increase of the 4f emission in the occupied density of states. The two weak structures at E_F and ~1.3 eV, attributed to 4f emission in $CePd_3$, become broader when boron is added to this compound. It is difficult to extract reliable information from these spectra since the presence of boron also modifies the shape of the Pd 4d density of states. The d-band maximum is shifted to higher binding energy by ~0.3 eV and its intensity relative to the shoulder at ~4 eV decreases. A similar concentration-dependent

change of the Au 5d band shape has been observed also in Au–Sn alloys by Friedman *et al* (1973). Moreover, in this system the increase of the Sn content induces in the same direction a shift of the valence band bottom. These effects were interpreted as a consequence of hybridisation of the Au 5d with the Sn sp valence band states. Similar effects could be responsible for the changes observed in the spectra of figure 1. Only a direct comparison with the isostructural compound $LaPd_3B_x$ could help us to extract safely the 4f emission from the valence band spectra of $CePd_3B_x$.

The influence of the boron sp states is also clearly visible in the unoccupied part of the valence bands. Apart from the decrease of the $4f^1$ emission with increasing boron concentration, the intensity of two structures deriving from Ce 5d states is attenuated. This behaviour can be expected, since these structures do not form in the presence of sp bands (Hillebrecht *et al* 1983), as demonstrated, for example, by the BIS spectrum of $CeAl_3$ (Baer *et al* 1981).

Furthermore, we note a shift of the 4f multiplet towards the Fermi energy on addition of boron. We interpret this behaviour as a manifestation of the increase of 4f occupation which is concomitant with a lowering of the 4f energies (Lang *et al* 1981).

3.2. Core levels

The decrease of the BIS $4f^1$ peak on addition of boron should have its counterpart in a corresponding decrease of the $4f^0$ component in the XPS 3d core level spectra. The structures of these spectra, shown in figure 2, have been interpreted in the conventional way (Fuggle *et al* 1983c) as indicated by the bar diagram below the XPS spectra. The expected f^0 intensity decrease for increasing boron concentration is very clearly observed. We shall attempt later to relate with the GS model these intensity variations of the spectroscopic signals with the lattice expansion.

For the moment it should be noticed that the strongest f^0 component is observed in $CePd_3$ at 90 K. This result is in glaring contradiction with the disappearance of the $4f^0$ signal at low temperature reported by Krill *et al* (1980). We suppose that the ion sputtering used by these authors to clean the sample surface has been performed at the different measurement temperatures. At low temperature the sample cannot recover from the structural disorder and ion implantation resulting from this treatment. In the damaged surface layers the mean interatomic Ce–Ce distances are certainly enlarged so that the Ce atoms are in a similar environment as in $CePd_3B_x$ compounds where the $4f^0$ XPS signal vanishes. We have also observed this manifestation of disorder in samples scraped at low temperature. For this reason we have cleaned the surface at room temperature before cooling and recording the low temperature spectrum of $CePd_3$ shown in figure 2.

We shall now attempt to extract from the weights of the different f^n signals observed in BIS and XPS the ground-state population n_f of the f level and its coupling Δ to the conduction electrons. We shall use the results of a model calculation proposed recently by Gunnarsson and Schönhammer (1983b). This formalism has been shown to be a powerful tool for analysing the spectra of a number of Ce compounds (Fuggle *et al* 1983a, c). Moreover, with the same set of ground state parameters, it has predicted correctly the evolution of XPS, BIS and EELS spectra through the γ–α phase transition of Ce metal (Wuilloud *et al* 1983). Within this model the coupling Δ is obtained from the intensity ratio $f^2/f^1 + f^2$ in the XPS spectra. Using figures 5 and 6 of Fuggle *et al* (1983c), where the dependence of this ratio of n_f and Δ is given, we obtain for all compounds studied here the same $\Delta = 150 \pm 20$ meV (see table 1), in agreement with the value

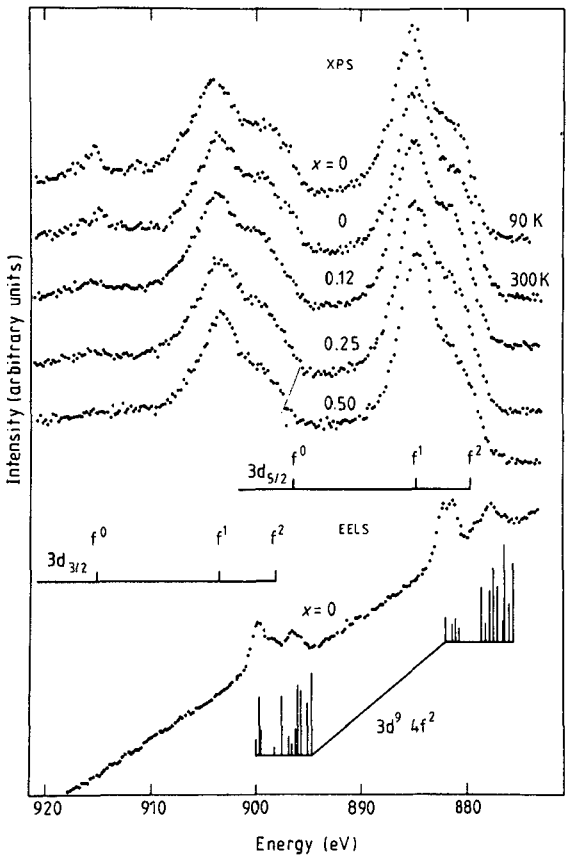

Figure 2. XPS and EELS 3d core level spectra of $CePd_3B_x$ for various concentrations x and temperatures T(K). The corresponding final states are indicated by the bar diagrams. For EELS the $3d^94f^2$ final state multiplet is taken from Spector *et al* (1976).

derived for $CePd_3$ in a previous study (Fuggle *et al* 1983c). However, we want to stress that, as a consequence of the partial overlap of the $3d^94f^1$ and $3d^94f^2$ final states, the determination of Δ is in fact more uncertain than usually assumed.

To illustrate this fact we present the EELS spectrum of the 3d core excitation region of $CePd_3$ in the bottom of figure 2. The observed structures correspond to the final $3d^94f^2$ configuration (Wuilloud *et al* 1983, Matthew *et al* 1983), the multiplets are indicated by the corresponding bar diagrams (Spector *et al* 1976). The comparison of XPS and EELS spectra shows that the superposition of the two final-state configurations makes the separation of their corresponding intensities in the XPS spectra rather hazardous, so that the proposed analysis can yield only a lower limit for Δ. The situation seems to be even more complicated: in the course of our study of Ce metal and several of its intermetallics we observed that the relative intensity distribution among the *individual* $3d^94f^2$ and $3d^94f^1$ multiplet terms can vary in the different compounds. For instance in γ-Ce the low binding energy shoulder in the XPS core level spectrum coincides with the dipole-forbidden transition region of the EELS $3d^94f^2$ multiplet (Wuilloud *et al* 1983). In $CePd_3$ however, the low binding energy component in the XPS spectrum corresponds to the dipole-allowed transition region observed in EELS. This peculiar behaviour might indicate that term-dependent f valence electron hybridisation leads to different transition

Table 1. Lattice constants, peak intensity ratios (as determined by BIS and XPS core level spectroscopy), f occupation probability, ($W(f^0)$) and 4f conduction electron hybridisation Δ for $CePd_3B_x$ compounds. $W(f^0)$ and Δ are derived on the basis of the Gunnarsson–Schönhammer model.

Compound	Lattice constant a(Å)	XPS $\frac{f^0}{f^0+f^1+f^2}$	BIS $\frac{f^1}{f^1+f^2}$	XPS $W(f^0)$	BIS $W(f^0)$	Δ (meV)
$CePd_3$ (90 K)	4.108†	0.075	—	0.109	—	150 ± 20
$CePd_3$ (300 K)	4.122† 4.124‡	0.053	0.174	0.084	0.078	150 ± 20
$CePd_3B_{0.12}$	4.156‡	0.020	0.073	0.031	0.026	150 ± 20
$CePd_3B_{0.25}$	4.186‡	0.015	0.049	0.015	0.013	150 ± 20
$CePd_3B_{0.5}$	4.203‡	~0.0	~0.0	~0.0	~0.0	150 ± 20
$CePd_3B$	4.203‡	—	—	—	—	—

† Harris and Raynor (1965).
‡ Dhar *et al* (1981).

probabilities for each multiplet term in the XPS spectra. This fact would lead to further complications in the derivation of Δ.

For the moment we shall keep the value of 150 meV obtained by our simple analysis in order to calculate the f ground-state occupation. Using figure 7 of Gunnarsson and Schönhammer (1983b), where the ratios $f^0/(f^0+f^1+f^2)$ (XPS) and $f^1/(f^1+f^2)$ (BIS) as a function of the initial f occupation are given for $\Delta = 120$ meV, we obtain the values summarised in table 1, columns 5 and 6. $W(f^0)$ is the probability for the f state to remain unoccupied. One should notice that for both spectroscopies the GS model yields rather consistent values. The BIS measurements, however, yield systematically smaller values than the ones obtained from the XPS core level spectra. By comparing the lattice constants with the derived f occupation (see table 1) one observes that a ~2% change in lattice spacing corresponds to a ~10% change in the f occupancy. We shall now attempt to derive a more general relationship between latttice expansion and f occupation for the compound $CePd_3B_x$.

3.3. Lattice expansion and f occupation

The f contribution to the cohesive energy depends on the lattice parameter through the hopping matrix element which increases on lattice contraction. Because of this attractive force due to f admixture in the ground state one has a contracted lattice compared with the case without valence instability.

We assume a power law for the dependence of the hopping matrix element, following Harrison (1980). We vary the parameter for the bare f level position ε_f and leave the other parameters entering the Anderson Hamiltonian constant. For the lattice parameter a at maximum cohesive energy we have

$$a - a_0 = -b\,\partial(\Delta E)/\partial a, \tag{1}$$

where a_0 denotes the lattice parameter, if the f electron does not contribute to cohesion, b is proportional to the reciprocal bulk modulus and ΔE denotes the lowering of the ground-state energy due to the f admixture. This effect does not depend linearly on the average f occupation n_f. Rather if ε_f is near the Fermi energy, n_f is near ≈ 0.5 and the

contraction is maximal. We have thus a non-linear variation with the f occupation n_f. To apply this theory to $CePd_3B_x$ we evaluated $\partial(\Delta E)/\partial a$ for a rectangular shape of the conduction band with lower band edge $-B$. We can express the result in a convenient form

$$(a - a_0)/(a_0\nu) = \text{constant} \times \Delta E(\varepsilon_f)W(f^0), \tag{2}$$

i.e. the lattice contraction is given essentially in terms of the product of the f-position-dependent lowering of the ground-state energy with the f occupation probability. We

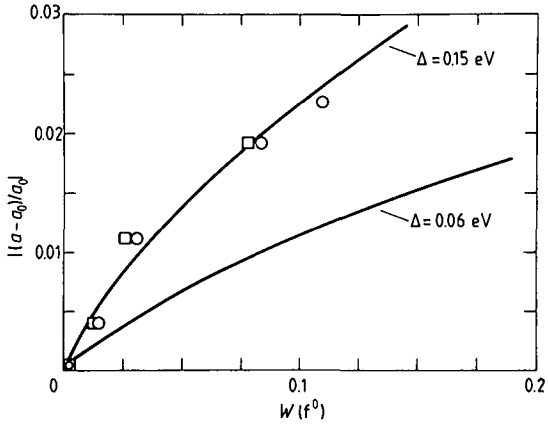

Figure 3. Lattice contraction versus f occupation for CeP_3B_x. The open circles and squares represent the experimentally derived XPS and BIS f occupancies, respectively. The full curves correspond to a calculation (see text) for two values of the f conduction electron hybridisation Δ.

have plotted equation (2) in the region of the experimentally determined occupancies in figure 3 for two values of $\Delta = N_f V^2$ where $N_f = 14$. We used $a_0 = 4.203$ Å ($CePd_3B_{0.5}$); and $B = 2$ eV for our choice of the conduction band. Since it is difficult to give an exact value for the power ν, we set $\nu = 6$ (Gunnarsson and Schönhammer 1983b).

The non-linear relationship between lattice contraction and f occupation is evident from this figure. Furthermore, the influence of Δ on the lattice contraction becomes obvious: for a given f occupation an increase in Δ, which is proportional to the hopping matrix element, leads to an increase in the lattice contraction. How do the experimentally determined f occupancies fit into this model? In view of the unknown power and bulk moduli we can only expect a qualitative agreement of the data with this model. We have indicated in figure 3 at the corresponding lattice constant differences the experimentally determined XPS and BIS intensity ratios (columns 5 and 6 of table 1) by the open circles and squares, respectively. We observe that the data follow nicely the theoretical curve corresponding to an experimentally found value of $\Delta = 150$ meV. Thus we have shown that for $CePd_3B_x$ (i) the GS model can be used confidently to extract ground state f occupation numbers from different spectroscopic techniques and (ii) that the f occupation changes on addition of boron can be successfully correlated with the non-linear increase of the lattice constant.

4. Summary

The intermetallic compound system $CePd_3B_x$ has been studied by XPS, BIS and EELS. As a function of the boron concentration strong variations of the occupied and empty parts

of the valence bands as well as of the 3d core levels are observed. The spectroscopic results were analysed consistently within the GS model. The boron-concentration-dependent lattice expansion was found to be correlated with an increase in f occupation from $n_f \simeq 0.9$ in $CePd_3$ to $n_f \simeq 1$ in $CePd_3B_{0.5}$, whereas the f conduction electron hybridisation remained at a value of $\Delta = 150 \pm 20$ meV for all compounds. A few problems connected with the derivation of Δ from spectroscopic data were also discussed. Furthermore, a non-linear dependence between the lattice expansion and f occupation is found in this compound system which is well accounted for by a calculation performed within the GS model.

Acknowledgment

This work has been supported by the Swiss National Science Foundation.

References

Allen J W, Oh S J, Lindau I, Lawrence J M, Johansson L I and Hagström S B 1981 *Phys. Rev. Lett.* **46** 1100
Baer Y, Ott H R, Fuggle J C, DeLong L E 1981 *Phys. Rev.* B **24** 5384
Croft M, Weaver J H, Peterman D J and Franciosi A 1981 *Phys. Rev. Lett.* **46** 1104
Dhar S K, Malik S K and Vijayaraghavan R 1981a *Phys. Rev.* B **24** 6182
—— 1981b *Mater. Res. Bull.* **16** 1557
Falicov L M, Hanke W and Maple M B 1981 *Valence Fluctuations in Solids* (Amsterdam: North-Holland)
Friedman R M, Hudis J, Perlman M L, Watson R E 1973 *Phys. Rev.* B **8** 2433
Fuggle J C, Hillebrecht F U, Esteva J M, Karnatak R C, Gunnarsson O and Schönhammer K 1983a *Phys. Rev.* B **27** 4673
Fuggle J C, Hillebrecht F U, Zeller R, Zolnierek Z, Bennett P A, Freiburg Ch 1983b *Phys. Rev.* B **27** 2145
Fuggle J C, Hillebrecht F U, Zolnierek Z, Lässer R, Freiburg Ch, Gunnarsson O and Schönhammer K 1983c *Phys. Rev.* B **27** 7330
Fujimori A 1983 *Phys. Rev. B* **28** 2281
Gunnarsson O and Schönhammer K 1983a *Phys. Rev. Lett.* **50** 604
—— 1983b *Phys. Rev.* B **28** 4315
Gupta L C, Sampathkumaran E V, Vijayaraghavan R, Hedge M S and Rao C N R 1980 *J. Phys. C: Solid State Phys.* **13** L455
Harris I R and Raynor G V 1965 *J. Less Common Met.* **9** 263
Harrison W A 1980 *Electronic Structure and the Properties of Solids* (San Francisco: Freeman)
Hillebrecht F U, Fuggle J C, Sawatzky G A and Zeller R 1983 *Phys. Rev. Lett.* **51** 1187
Holland-Moritz E, Loewenhaupt M, Schmatz W and Wohlleben D K 1977 *Phys. Rev. Lett.* **38** 983
Hüfner S and Steiner P 1982a *Z. Phys.* B **46** 37
—— 1982b *Valence Instabilities* ed. P Wachter and H Boppart (Amsterdam: North-Holland) p 263
Hüfner S, Steiner P, Dose V, Straub D and Härtl A 1983 *Solid State Commun.* **48** 257
Koenig C 1983 *Z. Phys.* B **50** 33
Krill G, Abadli L, Ravet M F, Kappler J P and Meyer A 1980 *J. Physique* **41** 1121
Lang J K and Baer Y 1979 *Rev. Sci. Instrum.* **50** 221
Lang J K, Baer Y and Cox P A 1981 *J. Phys. F: Met. Phys.* **11** 121
Laubschat C, Kaindl G, Sampathkumaran E V and Schneider W-D 1984 *Solid State Commun.* **49** 339
Lawrence J M, Riseborough P S and Parks R D 1981 *Rep. Prog. Phys.* **44** 1
Liu S H and Ho K-M 1982 *Phys. Rev.* B **26** 7052
Mårtensson N, Reihl B and Parks R D 1982 *Solid State Commun.* **41** 573
Matthew J A D, Strasser G and Netzer F P 1983 *Phys. Rev.* B **27** 5839
Moser H R 1983 *PhD Thesis* No 7369, ETH Zürich
Peterman D J, Weaver J H and Croft M 1982 *Phys. Rev.* B **25** 5530
Spector N, Bonelle C, Dufour G, Jørgensen C K and Berthou H 1976 *Chem. Phys. Lett.* **41** 199
Wachter P and Boppart H 1982 *Valence Instabilities* (Amsterdam: North-Holland)
Wuilloud E, Moser H R, Schneider W-D and Baer Y 1983 *Phys. Rev.* B **28** 7354

Physica 130B (1985) 144
North-Holland, Amsterdam

BORON-INDUCED CHANGES IN THE ELECTRONIC STRUCTURE OF $CePd_3$*

W.-D. SCHNEIDER, E. WUILLOUD, B. DELLEY and Y. BAER
Institut de Physique, Université de Neuchâtel, CH-2000 Neuchâtel, Switzerland

F. HULLIGER
Laboratorium für Feskörperphysik, ETH Zürich, CH-8093 Zürich, Switzerland

We report on high-energy spectroscopic measurements of the intermetallic rare earth compound system $CePd_3B_x$, with $0 < x < 0.5$. The combination of X-ray photoemission (XPS), Bremsstrahlung Isochromat (BIS) and electron energy loss (EELS) spectroscopies provides a powerful tool for studying the spectral changes of occupied and empty electronic states as a function of the boron concentration. In particular, upon boron addition a concomittant population decrease of the unoccupied Ce $4f^1$ as well as of the corresponding Ce $3d^9 4f^0$ core level final states is observed. These findings are fully consistent with the results of earlier lattice parameter and susceptibility measurements [1] and can be interpreted as resulting from a valence change of Ce from a mixed valent state in $CePd_3$ to a trivalent state in $CePd_3B_{0.5}$. An analysis of the spectroscopic results within the framework of the Anderson impurity model [2] shows that the boron concentration dependent lattice expansion induces a non-linear increase of the f-occupation number from $n_f \approx 0.9$ in $CePd_3$ to $n_f \approx 1$ in $CePd_3B_{0.5}$. Thus, as a consequence of the large values of the f conduction-electron hybridization $\Delta = 150 \mp 20$ meV [3], found for the whole compound series, this modest population increase can evidently cause a sizable lattice expansion. This behaviour indicates clearly the participation of f-electrons to the chemical bond [2].

The localized and/or bonding states of f-symmetry seem to be both responsible for the appearance of different local f-populations in the core level spectra of RE and actinide compounds [4, 5, 6]. It is argued that the initial hybridization can be broken by the strengthening of the atomic potential resulting from the presence of a core hole. Since the observed intensity distribution between the various final states is well accounted for by the Gunnarsson–Schönhammer model [2] in rare earth systems, it is suggested that this formalism should also be applicable to actinide systems with weak f-wave function overlap.

* A full version of this paper will appear in J. Phys. C: Solid State Phys. 17 (1984) 4799.

References

[1] S.K. Dhar, S.K. Malik and R. Vijayaraghavan, Phys. Rev. B24 (1981) 6182.
[2] O. Gunnarsson and K. Schönhammer, Phys. Rev. B28 (1983) 4315.
[3] For $CePd_3$ this value is in excellent agreement with an earlier determination by J.C. Fuggle, F.U. Hillebrecht, Z. Zolnierek, R. Lässer, Ch. Freiburg, O. Gunnarsson and K. Schönhammer, Phys. Rev. B27 (1983) 7330.
[4] Y. Baer, H.R. Ott and K. Andres, Solid State Commun. 36 (1980) 387.
[5] W.-D. Schneider and C. Laubschat, Phys. Rev. Lett. 46 (1981) 1023.
[6] E. Wuilloud, B. Delley, W.-D. Schneider and Y. Baer, Phys. Rev. Lett. 53 (1984) 202.

Spectroscopic Evidence for Localized and Extended f-Symmetry States in CeO_2

E. Wuilloud, B. Delley, W.-D. Schneider, and Y. Baer
Institut de Physique, Université de Neuchâtel, CH-2000 Neuchâtel, Switzerland
(Received 1 March 1984)

The occupied and empty electronic states of the insulator CeO_2 have been studied by high-energy spectroscopies. The outer-level spectra reveal empty localized $4f^1$ states within the band gap. The core-level spectra display different final-state populations of the $4f$ localized states which are well predicted by a many-body calculation taking into account the presence of f-symmetry admixture in the valence band. A mixed valence can be definitely excluded in CeO_2.

PACS numbers: 71.70.Ms, 79.20.Kz, 79.60.Eq

The electronic structure of Ce metal and its intermetallic compounds has been and continues to be a very fascinating research area offering the best accessible possibility to investigate the consequences of the degeneracy between extended states of a metallic band and an atomiclike localized $4f$ state. Obviously, this situation cannot be described as a conventional hybridization since, despite their strong interaction, these two kinds of states keep to a large extent their respective extended and localized character. The resulting many-body states seem to be correctly accounted for in the framework of the Anderson impurity model, and the computation of the response of such systems to very different spectroscopic excitations shows encouraging agreement with the experimental spectra.[1-3]

In an ionic compound like CeO_2, a new situation can be anticipated, which is different from the one met in Ce intermetallics studied so far. This fact is best demonstrated by the controversial opinions concerning the ground-state properties of this insulating compound. The observation of distinct L_{III} x-ray absorption edges of Ce has been interpreted as evidence of an initial $4f^0 \leftrightarrow 4f^1$ mixed-valent state.[4] However, this description has been called into question on the basis of optical and magnetic properties, reflecting the insulating character of this compound. A simpler picture of a formally full oxygen $2p$ band and a tetravalent ($4f^0$) configuration of the Ce atoms was proposed.[5] Later on a specific local valence-mixing mechanism between O $2p$ and Ce $4f$ states was attempted in order to reconcile mixed-valence behavior (deduced from core-level spectra) with the insulating properties of this material.[6] A very recent self-consistent-field band calculation of the electronic structure of CeO_2 indicates clearly that this compound is an insulator with a band gap of 6 eV.[7] A careful symmetry analysis of the ground-state eigenfunctions shows that the states of nearly pure $4f$ localized character remain unoccupied ($n_f^{\downarrow}=0$) in the band gap whereas the valence-band states contain a nonnegligible admixture of f symmetry ($n_f^{\downarrow}>0$) with an extended radial behavior.[7] The aim of the present work is to test the compatibility of this ground-state description with the results obtained by different spectroscopies. A model calculation[1] taking into account the relevant aspects of this initial state has been performed in order to predict the different experimental spectra.

The spectra presented in this investigation were obtained in a spectrometer which allows us to perform x-ray photoelectron spectroscopy (XPS), bremsstrahlung isochromat spectroscopy (BIS), and electron energy-loss spectroscopy (EELS) on the same sample without breaking the base pressure of 1×10^{-11} Torr.[8,9] The CeO_2 sample was prepared *in situ* from metallic Ce films evaporated on graphite and oxidized at 800 K in an oxygen atmosphere of 1 Torr for 6 h. The check of the CeO_2 purity by monitoring the XPS O $1s$ signal yielded an upper limit of 5% for the presence of lower oxides. The electron bombardment of the surface in BIS and EELS was found to induce a fast surface reduction of CeO_2 to Ce_2O_3. This instability could be widely eliminated by exposing the sample to an oxygen atmosphere of 1×10^{-8} Torr[10] during the measurements. By varying the electron-beam current from 50 to 200 μA, no charging effect of the thin CeO_2 film could be detected. The outer-level energies in XPS and BIS spectra were calibrated with respect to the sample Fermi level determined within ±0.1 eV by measuring a Au film deposited by evaporation onto CeO_2.

Figure 1 shows the occupied and empty density of states (DOS) of CeO_2 as obtained from the joined XPS and BIS spectra. Our XPS spectrum confirms an earlier result measured with a lower resolution on a pressed CeO_2 powder sample.[11] As far as we know, no BIS spectrum of pure CeO_2 has been published.[12] The agreement between the experimental spectra of Fig. 1 and the density of the

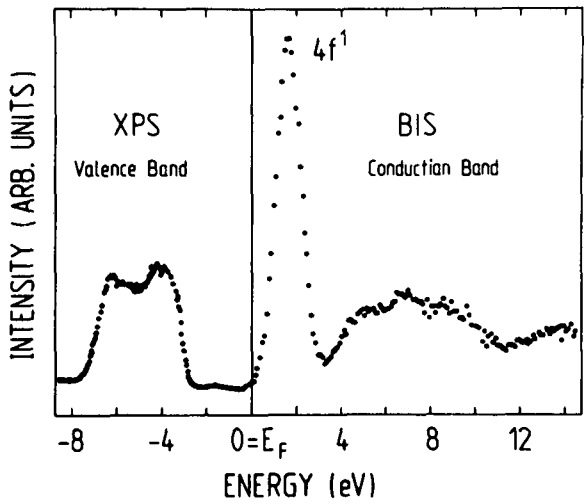

FIG. 1. Combined XPS-BIS spectrum of CeO_2.

ground-state eigenvalues shown in Fig. 2 of Ref. 7 is striking. The XPS valence band of mainly $2p$ character confirms the existence of many predicted fine structures. In the BIS spectrum, by extrapolation of the conduction band below the main peak, a band gap of ~ 6 eV is determined in good agreement with the calculation. The BIS spectrum displays also an upper edge delimiting probably an 8-eV-broad $6d$ band. The prominent peak located in the band gap represents unambiguously the single occupation of the initially empty $4f^0$ states. The measured full width at half maximum of 1.2 eV of this resonance is compatible with a $4f_{7/2,5/2}$ spin-orbit doublet convolved with two Gaussians of ~ 0.6 eV width representing the instrumental resolution and lifetime broadening.[13] This observation points out the localized character of these empty states. The position of the $4f^1$ excitation relative to the extended states is qualitatively in agreement with the computed position of the $4f$ state. However, for highly correlated $4f$ electrons the ground-state eigenvalues do not represent precisely the measured energies. From the spectra of samples containing a substantial mixture of CeO_2 and Ce_2O_3 we have clearly observed the XPS $4f^1$ and BIS $4f^2$ final states of Ce_2O_3 at -1.6 and 7 eV, respectively (barely discernible contributions can be recognized in the spectra of Fig. 1). It seems reasonable to assume similar screening mechanisms in the two oxides so that the $4f^1$-$4f^2$ energy separation is roughly the same in both cases. Thus, if there *were* any occupation of the local level, an additional $4f^2$ structure in the BIS spectrum would be expected at 10 eV, not far below the upper band edge; and if there were local f character in the valence band, additional structure would be expected near the lower

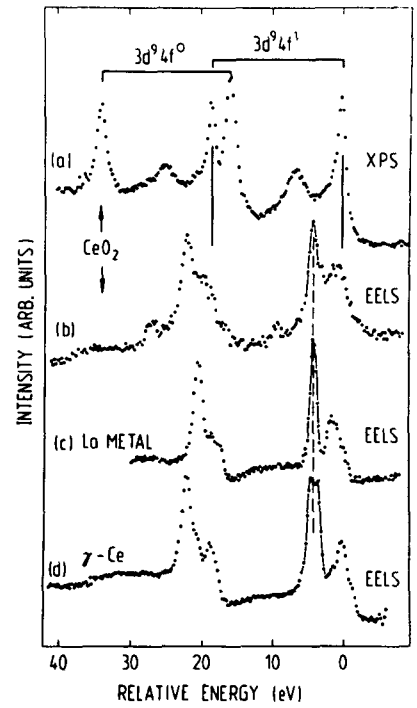

FIG. 2. (Curve *a*) XPS and (curve *b*) EELS spectra of $3d$ core excitations in CeO_2 on a common energy-loss scale. The spectra for (curve *c*) La and (curve *d*) γ-Ce are aligned.

conduction band edge. That no such $4f^2$ structures are observed attests to the fact that the local $4f$ states are completely unoccupied, in agreement with the ground-state calculation. The predicted existence of f mixing in the bands[7] cannot be directly recognized in the outer-level spectra but will be found to play an essential role in the coupling with the different core-hole final states.

The creation of a core hole destroys locally the translational symmetry by enhancing the potential of a particular atom. The extended band states are only weakly affected while the localized $4f$ states suffer an important lowering of their energy. The final states of any core-level spectroscopy will reflect a locally completely different situation than in the initial state around the ionized atom. Furthermore, in the sudden approximation, the existence of f character mixed to the initial valence-band states is considered responsible for a sizeable coupling to the different localized $4f$ final populations. For the moment, we shall only attempt to identify the different final-state configurations observed in the XPS and EELS spectra shown on a common energy scale in Fig. 2. In an insulator, the most natural way to define for XPS an energy scale compatible with the energy losses in EELS is to take the upper band edge as origin. The well separated

structures observed in the XPS $3d$ spectrum shown in Fig. 2, curve a confirm an earlier result obtained on a CeO_2 powder sample.[14] In the EELS spectrum of CeO_2, the two well separated spin-orbit–split components show the typical multiplet structures of a $3d^9 4f^1$ final state. This identification is established by comparison with the EELS spectra of La and Ce which have been shown to correspond to $3d^9 4f^1$ and $3d^9 4f^2$ final states, respectively.[9,13] These spectra are represented in Fig. 2, curves c and d with one of their leading peaks aligned on the corresponding peak of CeO_2 (dashed line). The data points of these peaks have been connected with a line to guide the eye in order to make conspicuous the differences between the EELS spectra of CeO_2, La, and Ce. A careful inspection of these multiplet structures shows that the CeO_2 EELS spectum is nearly identical to the one of the La and in fact different from the one of Ce. We can take advantage of the detailed analysis of the La spectra[9] and attribute in CeO_2 the XPS final state observed in the corresponding energy range to $3d^9 4f^1$ atomiclike final states. The nature of the weaker structures occurring at higher energies in XPS and EELS is not obvious but is likely to have a pronounced $3d^9 4f^2$ character.[6] Finally, the intense XPS lines at the highest energies can be identified with the $3d^9 4f^0$ final state, since no corresponding EELS structures can be found. This final-state identification based on experimental observations is at variance with the assignment made in the calculation of Thornton and Dempsey[15] but in agreement with the one of Ref. 6. It is interesting to notice that the weakest EELS structures were already detected in an earlier photoabsorption measurement[16] but could not be interpreted. Thus far we have been able to identify the nature of the different excitations observed in core-level spectra, but their relative intensity distribution cannot be simply predicted since the coupling between initial and final states must be calculated in a many-body formalism simulating the situation encountered in CeO_2.

We have adapted the Gunnaarsson-Schönhammer GS model[1] to the case of an insulator by defining a full valence band of rectangular shape allowed to hybridize with an f level above it. With the parameter values given in Fig. 3 the weight of the $4f^1$ configuration in the ground state is about 0.5, in qualititative agreement with the self-consistent field calculation.[7] Since the computed XPS and BIS spectra shown in Fig. 3(a) represent excitation spectra accounting only for f-symmetry states they cannot be directly compared with the ground-state calculation of the total DOS.[7] For the extended

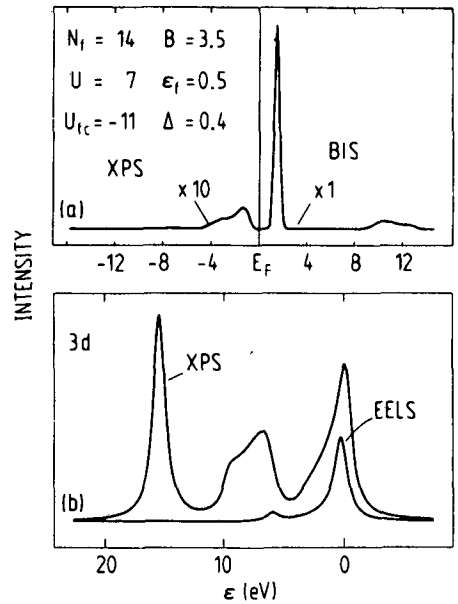

FIG. 3. Result of the many-body calculation for the different excitation spectra in CeO_2. (a) f contribution to the outer-level excitations. (b) $3d$ core excitations (see text). The spectra shown in (a) have been convoluted by a Gaussian of 0.4 eV full width at half maximum and those in (b) by a Lorentzian of 1.2 eV full width at half maximum. The parameters are defined as in Ref. 1.

states, however, the calculated f contribution to the exctitation spectra should be comparable to an f-projected DOS of a band calculation. As expected the f contribution in XPS is comparatively weak and broad. In the band gap the calculation predicts correctly the narrow resonance corresponding to the population of the localized $4f^1$ states. Since the model ignores the existence of a conduction band, instead of an f admixture to this band, it produces a rather unrealistic f^2 contribution. The same set of parameters producing excitation spectra of outer levels in good agreement with experiment has been used to calculate the core-level spectra shown in Fig. 3(b). The multiplet splitting which influences more strongly the EELS final-state structures has not been taken into account. With this simplification, the expected differences in the $3d \rightarrow 4f$ excitation processes between EELS and x-ray absorption spectroscopy, which are due to multiplet term-dependent matrix elements, have not been accounted for by the theory. In view of this omission and other approximations made in the model, it describes the XPS and EELS spectra surprisingly well. The calculated peaks in the XPS and EELS core-level spectra derive from the f^0, f^1, and f^2 final states in the limit of $V \rightarrow 0$ in the order of decreasing relative energy. However, at finite V, the

f^1, f^2 mixing impedes an unambiguous assignment. Finally, $2p \rightarrow 5d$ excitations (L_{III} edges), calculated within the same formalism, are in qualitative agreement with experiment.[4] The success of this formalism applied to the new situation encountered in CeO_2 provides a glaring demonstration that hybridized and extended f-symmetry states are also strongly coupled to deep-hole final states with different localized $4f$ populations.

This work has demonstrated that in CeO_2 the localized $4f$ states remain completely unoccupied whereas the proximity of the huge $4f$ resonance induces a nonnegligible $l=3$ projected DOS in the valence band. These extended covalent states with f symmetry are responsible for the coupling to core-hole final states with different populations of localized $4f$ levels. This observation is confirmed by a model calculation describing the different spectroscopic processes, and it establishes quite generally that discrete final states in core-level spectroscopies do not necessarily reflect an initial mixed-valence state. The angular momentum rather than the degree of localization appears to be the essential parameter driving the coupling between the outer states when a core hole is suddenly created. It can be anticipated that this deepening of the core-level spectra interpretation will provide a powerful tool for probing the symmetry character of the states participating in the bond.

This work was supported by the Swiss National Science Foundation. We are grateful to Hans Beck for stimulating discussions.

[1]O. Gunnarsson and K. Schönhammer, Phys. Rev. B **28**, 4315 (1983).

[2]J. C. Fuggle *et al.*, Phys. Rev. B **27**, 4637 (1983).

[3]J. C. Fuggle *et al.*, Phys. Rev. B **27**, 7330 (1983).

[4]K. R. Bauchspiess *et al.*, in *Valence Fluctuations in Solids*, edited by L. M. Falicov, W. Hanke, and M. B. Maple (North-Holland, Amsterdam, 1981), p. 147.

[5]P. Wachter, in *Valence Instabilities*, edited by P. Wachter and H. Boppart (North-Holland, Amsterdam, 1982), p. 145.

[6]A. Fujimori, Phys. Rev. B **28**, 2281 (1983).

[7]D. D. Koelling *et al.*, Solid State Commun. **47**, 227 (1983).

[8]J. K. Lang and Y. Baer, Rev. Sci. Instrum. **50**, 221 (1979).

[9]H. R. Moser *et al.*, Phys. Rev. B **29**, 2947 (1984).

[10]F. P. Netzer *et al.*, Phys. Rev. Lett. **51**, 211 (1983).

[11]A. F. Orchard and G. Thornton, J. Electron Spectrosc. Relat. Phenom. **10**, 1 (1977).

[12]S.-J. Oh *et al.*, Bull. Am. Phys. Soc. **28**, 269 (1983).

[13]E. Wuilloud *et al.*, Phys. Rev. B **28**, 7354 (1983).

[14]P. Burroughs *et al.*, J. Chem. Soc., Dalton Trans. **17**, 1686 (1976).

[15]G. Thornton and M. J. Dempsey, Chem. Phys. Lett. **77**, 409 (1981).

[16]C. Bonnelle *et al.*, Phys. Rev. A **9**, 1920 (1974).

Comment on "Spectroscopic Evidence for Localized and Extended f-Symmetry States in CeO_2"

In a recent Letter, Wuilloud, Delley, Schneider, and Baer (WDSB)[1] presented combined x-ray photoelectron spectroscopy and bremsstrahlung isochromat spectroscopy (BIS) studies of CeO_2 focusing on the possibility of valence mixing in this insulating compound, which has been a controversial issue for recent years.[2-4] They concluded that in CeO_2 f-symmetry states exist as extended states as calculated by band theory[5] and that valence mixing as proposed by the cluster model of Fujimori with configuration mixing[4] is definitely excluded. They argued that, whereas the valence band contains an admixture of f symmetry ($n_f^h \neq 0$), the occupancy of localized $4f$ states n_f^l is zero.

In this Comment, I would like to point out that their results are consistent with the valence mixing of Ref. 4 rather than excluding it. I note that the cluster model[4] and the band model[5] have given quite similar physical pictures in spite of the very different approaches as far as the ground state is concerned. While the band model considers the Ce $4f$–O $2p$ hybridization in a one-electron picture, the cluster model considers it in a configuration-mixing framework.[6] In both cases, $4f$ electrons are delocalized in the sense that they lose localized magnetic moments and participate in chemical bonding. In fact, their "extended f-symmetry states" can be regarded as linear combinations of O $2p$ and Ce $4f$ atomic orbitals as can be seen from the shape of the wave function in Ref. 5. Therefore, the conclusion of WDSB that $n_f^h \neq 0$ and $n_f^l = 0$ is fully consistent with the cluster-model results: The result of Ref. 4 that CeO_2 is mixed valent with $n_f \sim 0.6$ corresponds well to $n_f^h \sim 0.5$ used by WDSB in their model calculations.[1]

Then, which is a more relevant definition for the $4f$ occupancy, $n_f = n_f^l + n_f^h$ or n_f^l? Core-level[7] and valence-band[8] photoemission measures n_f rather than n_f^l. So-called tetravalent compounds such as $CeRh_3$ and $CeRu_2$, for which $n_f^l \sim 0$, have been assigned the $4f$ number of ~ 0.8.[7] The $4f$ occupancy measured by Compton scattering[9] also corresponds to n_f, as this experiment measures spatial electron distribution and does not distinguish localized, magnetic $4f$ electrons, and $4f$ electrons hybridized with conduction electrons. Generally it is not possible to separate unambiguously n_f into n_f^l and n_f^h in metallic Ce systems both experimentally and theoretically. Therefore we believe that n_f is a parameter more relevant to recent arguments on the $4f$ occupancy than n_f^l, and in this sense CeO_2 should be regarded as mixed valent, although the chemical term "valence" might be confusing.

Finally, the BIS spectrum of CeO_2 has shown an intense $4f^1$ peak and no clear $4f^2$ peak, which WDSB considered to be a strong indication of unoccupied localized $4f$ states. WDSB used a large $4f$-valence (conduction) band hybridization parameter in their Gunnarsson-Schönhammer (GS)[10] model calculations ($N_f\Delta = 5.6$ eV as compared to V or $N_f\Delta = 0.5$–2.5 eV used in the cluster calculations[4] and previous GS model calculations[7,10]). As a result of the large hybridization the intense BIS peak is an admixture of $4f^1$ and $4f^2$ configurations with comparable weight rather than pure $4f^1$, and cannot be assigned to localized $4f^1$ states. Alternatively, the intense "$4f^1$" peak might be explained by a formation of $4f$ band in the BIS final state,[11] which cannot be described by single-Ce-ion theories such as the GS and cluster models. In any case, unoccupied $4f$ states are fairly extended rather than localized.

I would like to thank Professor J. H. Weaver for encouragement and the National Science Foundation for support through Grant No. DMR 82-16489.

Atsushi Fujimori[a]
Department of Chemical Engineering and Materials Science
University of Minnesota
Minneapolis, Minnesota 55455

Received 27 August 1984
PACS numbers: 71.70.Ms, 79.20.Kz, 79.60.Eq

[a]Permanent address: National Institute for Research in Inorganic Materials, Sakura-mura, Niihari-gun, Ibaraki 305, Japan.

[1]E. Wuilloud *et al.*, Phys. Rev. Lett. **53**, 202 (1984).
[2]K. R. Bauchspiess *et al.*, in *Valence Fluctuations in Solids*, edited by L. M. Falicov, W. Hanke, and M. B. Maple (North-Holland, Amsterdam, 1981), p. 147.
[3]P. Wachter, in *Valence Instabilities*, edited by P. Wachter and H. Boppart (North-Holland, Amsterdam, 1982), p. 145.
[4]A. Fujimori, Phys. Rev. B **28**, 2281, 4489 (1983).
[5]D. D. Koelling *et al.*, Solid State Commun. **47**, 227 (1983).
[6]J. H. Hubbard *et al.*, Proc. Roy. Soc. London **88**, 13 (1960).
[7]J. C. Fuggle *et al.*, Phys. Rev. B **27**, 7330 (1983).
[8]D. J. Peterman *et al.*, Phys. Rev. B **27**, 808 (1983).
[9]U. Kornstädt *et al.*, Phys. Rev. B **21**, 1898 (1980).
[10]O. Gunnarsson *et al.*, Phys. Rev. B **28**, 4315 (1983).
[11]J. W. Allen *et al.*, Phys. Rev. B **28**, 5327 (1983).

Wuilloud *et al.* Respond: In the previous Comment on our electron spectroscopy study of CeO_2,[1] Fujimori criticizes concretely only the large hybridization energy and our characterization of the unoccupied f states. He rather attempts to argue that his cluster calculation is equivalent to our model calculation performed within the Anderson impurity model. He also maintains his opinion that the p-f mixing mechanism can be considered as a mixed valence. We disagree with the argumentation proposed by Fujimori.

In the cluster calculation of CeO_2,[2] the real electronic structure is approximated by the hybridization of an f state with a few ligand states in a tight-binding-type treatment. As a consequence, this model is definitely confined within an atomiclike description where the ground state and the excitations appear necessarily as discrete spectra of localized states (see Fig. 2 of Ref. 2). This approach to a solid is missing irremediably the continuum aspects of the band states interacting with the f state. For example, one unrealistic consequence of such a model is the fact that the lowest excitation energies are typically of the order of the hybridization energy for both metals and insulators. This implies zero electronic specific heat and too small susceptibilities for metallic systems.

In the present problem, the essential advantage of the impurity model is that it is specifically constructed to describe the interaction of an impurity level with a continuum of states. In contrast to the cluster model it is not limited to a localized description of the states.

CeO_2 offers a very clear situation when compared with metals since the valence and conduction bands consisting of extended Bloch states are separated by a gap. The peak observed in this gap above E_F in the BIS spectrum is well predicted by the impurity calculation which confirms that it has a nearly pure (90%) $4f^1$ character. The weak "f^2" structure is in fact a complicated mixture of f^2, and f^1–conduction electron–valence hole states. The impurity calculation yields an f admixture spread over the whole valence bandwidth being fully consistent with the old ideas on covalency. A cluster calculation can not distinguish between this bonding mechanism and a true mixed valence.

For the $3d$ core levels the impurity model shows that the lowest peak of each spin-orbit component has a rather pure f^0 character. However, the other structures correspond to a strong mixing where the f^1/f^2 ratio is of the order of 1 for each peak. The importance to include the continuum aspects of the valence states is demonstrated by a more realistic prediction of the core-level line shapes. In his cluster model Fujimori starts from fixed hybridization values 1.48 and 1.71 eV^2 and adjusts the theoretical core-level spectrum to experiment by varying the f-promotion energies. He obtains promotion energies E_1 and E_2 implying a screened Coulomb correlation energy $U_{ff} = 15$ eV.[2] Even in an insulator this values appears to be a factor of 2 larger than generally accepted and observed in Ce_2O_3.[1] It is not surprising that about the same f count n_f is obtained in both models. This results from the fact that the cluster model corresponds roughly to the impurity model in a zero bandwidth limit. The f count is mostly determined by the relative weights f^0/f^1+f^2 of the different core-level components, which do not depend critically on the bandwidth.

The Ce atoms in CeO_2 are tetravalent since no localized f level is occupied and the four outer electrons are involved in the band. In a cluster approach, the covalent f admixture to the band states can only be synthesized by mixing a limited number of localized orbitals. Therefore we believe that this approximation of a band has no common feature with the concept of mixed valence. The term mixed valence characterizes the fractional occupation of a localized state in a metal.[3]

E. Wuilloud
B. Delley
W.-D. Schneider
Y. Baer
Institut de Physique
Universite de Neuchatel
CH-2000 Neuchatel, Switzerland

[1]E. Wuilloud, B. Delley, W.-D. Schneider, and Y. Baer, Phys. Rev. Lett. 53, 202 (1984).
[2]A. Fujimori, Phys. Rev. B 28, 2281 (1983).
[3]C. M. Varma, Rev. Mod. Phys. **48**, 219 (1976).

Journal of Magnetism and Magnetic Materials 47&48 (1985) 197–199
North-Holland, Amsterdam

SPECTROSCOPIC STUDY OF LOCALIZED AND EXTENDED f-SYMMETRY STATES IN CeO_2, CeN AND $CeSi_2$

E. WUILLOUD, B. DELLEY, W.-D. SCHNEIDER AND Y. BAER

Institut de Physique, Université de Neuchâtel, CH-2000 Neuchâtel, Switzerland

The occupied and empty electronic states of CeO_2, CeN and $CeSi_2$ have been studied by high-energy spectroscopies (XPS, BIS). The experimental results are remarkably well predicted by a many-body calculation accounting for f-symmetry admixture in the bands. The compounds CeN and $CeSi_2$ can be considered as mixed valent while this phenomenon can be definitely excluded in CeO_2.

The interaction of an atomic-like electronic state with extended band states located in the same energy region offers an exceptional situation which can give rise to many attractive phenomena like Kondo effect, valence instabilities and most likely the heavy-fermion behaviour recently discovered in Ce-and U-based intermetallics. The unusual electronic properties of these systems have already been the subject of numerous spectroscopic studies interpreted with very different and sometimes controversial models. The modified Anderson impurity model including a large f-orbital degeneracy proposed by Gunnarsson and Schönhammer (GS) [1,2] appears to provide at the present moment the most successful method for calculating very different excitation spectra (XPS, BIS, XAS, EELS) with the same set of parameters characterizing the sample. It has been mostly applied to alloys of Ce with d-metals [3–5]. The purpose of this study is to compare GS model calculations with spectroscopic results of systems where the 4f-state interacts with a band originating from p-states [6,7]. This symmetry offers more freedom than d-states to vary drastically the density of the extended states in the energy range of the $4f^1$ resonance. We have choosen to investigate the sequence CeO_2, CeN and $CeSi_2$, where the p–d gap shrinks from 6 to ≈ 0 eV.

The experimental results presented in this paper were obtained in a combined XPS (X-ray Photoelectron Spectroscopy), BIS (Bremstrahlung Isochromat Spectroscopy) and EELS (Electrons Energy Loss Spectroscopy) apparatus allowing us to perform all measurements in a vacuum of 2×10^{-11} Torr. The CeO_2 and CeN samples were prepared in situ from metallic Ce-films evaporated on graphite. In order to obtain the compounds, these films were heated at 800 K during 6 h expositions to 1 Torr oxygen or 760 Torr nitrogen pressures, respectively. The polycrystalline sample of $CeSi_2$ was prepared by melting the stoichiometric amounts of Ce and Si in a levitation furnace and, subsequently, by tempering it at 800 K. Within the X-ray detection limit, the sample was found to form a single phase.

The joined XPS and BIS spectra shown in fig. 1

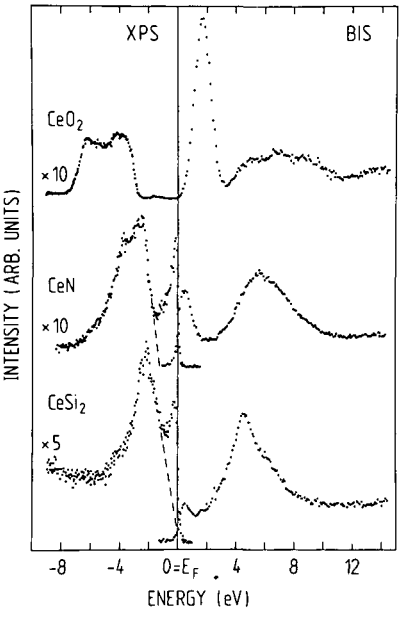

Fig. 1. Combined XPS–BIS spectra of CeO_2, CeN and $CeSi_2$. The relative intensities have been normalized (see text). The extrapolated upper valence band edges are indicated by the dashed lines.

display the occupied and empty densities of states of CeO_2, CeN and $CeSi_2$. The spectra of CeO_2 have already been published elsewhere [8], the thin-film XPS spectrum of CeN is in perfect agreement with a previous spectrum of a CeN single crystal [9] and $CeSi_2$ has only been studied by resonant photoemission [10]. The relative intensities of the different spectra have been tentatively adjusted by using the computed atomic cross-section for the different symmetries [11]. For CeO_2, the populations obtained in a band calculation [12] have been used, for CeN and $CeSi_2$, this kind of information being not available, only the 4f contributions have been adjusted to the populations predicted by the many-body calculation presented later in this paper.

The XPS, BIS and EELS spectra of CeO_2 have been interpreted with a GS model adapted to an insulator and compared to a SCF band calculation [12]. This study has provided an unquestionable demonstration that an important participation of f-symmetry is involved in the extended states forming the band while no localized 4f-state is occupied. As shown in fig. 1, the 4f resonance is located above E_F within the band gap and therefore can remain essentially atomic-like. The many-body analysis of the core levels, (not shown here) requires for the coupling Δ between 4f and valence states the very large value of 0.4 eV. The consequence is an important f admixture of 0.5 states in the "p" band as shown in fig. 2 by the projected f-density of states obtained in the many-body calculation. In CeO_2 the new situation results from the presence of a large band gap allowing the energy separation of hybridized and localized contributions of the f-states. The tetravalence of this oxide is demonstrated by the fact that the BIS spectrum shows simply a $4f^1$ peak below the empty band which cannot be confused with $4f^2$ multiplets.

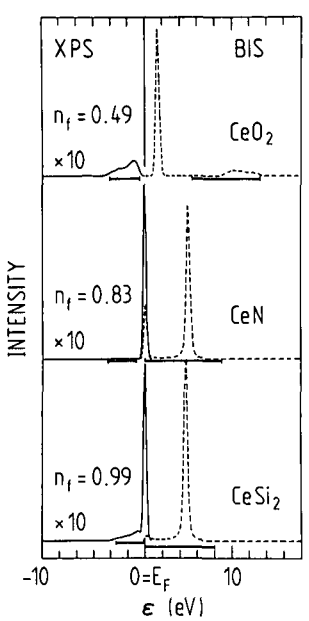

Fig. 2. Result of a many-body calculation for the f contribution to the excitation spectra of the outer occupied (full curve) and empty (dashed line) states for CeO_2, CeN and $CeSi_2$. The total f occupation n_f is indicated. The parameters are defined as in refs. [1,2] (see text). The positions and widths of the semi-elliptical valence and conduction band states are indicated by the horizontal bars.

In CeN only 3 electrons of the Ce atoms are necessary to complete the p band of N. In the XPS spectrum of fig. 1, by extrapolation the upper valence band edge is found to be located about 1.5 eV below E_F, so that a narrower p–d band gap than in CeO_2 is formed. The $4f^1$-state must be assumed here to overlap weakly with the d-conduction band (fig. 2). This description is dictated by the choice of parameters producing the best agreement of the many-body calculation with the core level and 4f excitations. In the XPS spectrum, the tail of the $4f^1$ peak toward the p band is likely to be attributed to the localized $4f^1$ level shifted at the surface, as observed at lower photon energies [13]. The weak energies of 0.1 and 0.05 eV found for the coupling of valence and conduction electrons with the 4f states as well as the 4f separation from the upper valence band edge are responsible for the 4f localization. This situation is illustrated in fig. 2 by a barely discernable hybridized f contribution. The degeneracy of the localized $4f^1$ level with the conduction band causes a fractional occupation ($n_1^f \approx 0.8$) of the localized $4f^1$-state, a phenomenon usually called valence fluctuation. This situation is confirmed by the BIS spectrum of fig. 1 showing above the $4f^1$ peak the typical structure corresponding to the population of the $4f^2$ multiplets. These states of localized nature are resonantly bound in the potential well; their multiplet splitting has not been included in the many-body calculation and only the area of the corresponding 4f signals must be compared in theory and experiment.

In $CeSi_2$ the estimation of the upper p-band edge (dashed line) indicates that this compound looks rather like a semi-metal with the $4f^1$-state squeezed in the DOS minimum between the conduction and the valence band. The fit of the many-body calculation to the spectra yields practically the same coupling energies between 4f and band states as those found for CeN. However, in this case the bare $4f^1$ energy is found to be located 0.25 eV below E_F in the valence band. It results that the 4f occupation n_f is nearly equal to one and that, besides the occupied 4f peak just below E_F and accounting for

localized states (n_l^f), a sizable f admixture (n_h^f) to the p band is predicted by the calculation. The measured and computed spectra corresponding to the addition of a 4f electron (BIS) reflect also clearly that the intermediate valence of Ce in $CeSi_2$ is not far from the trivalence. This conclusion is confirmed by the occurrence of magnetic transitions for compositions with Si deficiency [14,15]. This stiochiometry change appears to push the $4f^1$ state further below E_F and to induce the integral occupation $n_l^f = 1$. The interpretation of resonant photoemission spectra proposed earlier [10] is completely at variance with the present description of the $CeSi_2$ electronic structure. The changes in the $4f^2$ multiplet shape and position from CeN to $CeSi_2$ are quite similar to the observation made in the $CePd_3B_x$ series [16] and therefore can be interpreted as a manifestation of the 4f occupation increase.

The analysis by the GS model of this class of Ce compounds can not discriminate numerically between localized (n_l^f) and hybridized (n_h^f) f occupations but these two kinds of contributions can be distinguished by their different width and shape in the calculated excitation spectra of the outer levels (see fig. 2). The intensity ratio of the different structures in all kinds of spectra have no longer a linear dependence on the total number of occupied f-symmetry states $n_t^f = n_l^f + n_h^f$. These facts obviously invalidate any simplistic valence determination from core level spectra when Δ is sizeable. For example the set of parameters used to analyze the present CeO_2 spectra allows us to compute a L_{III} absorption edge [17] in satisfactory agreement with an experimental spectrum from which a fractional valence of the Ce atom in this oxide was deduced [18].

References

[1] O. Gunnarsson and K. Schönhammer, Phys. Rev. Lett. 50 (1983) 604.

[2] O. Gunnarsson and K. Schönhammer, Phys. Rev. B28 (1983) 4315.

[3] J.C. Fuggle, F.U. Hillebrecht, Z. Zolnierek, R. Lässer, Ch. Freiburg, O. Gunnarsson and K. Schönhammer, Phys. Rev. B27 (1983) 7330.

[4] J.C. Fuggle, F.U. Hillebrecht, J.M. Esteva, R.C. Karnatak, O. Gunnarsson and K. Schönhammer, Phys. Rev. B27 (1983) 4637.

[5] F.U. Hillebrecht, J.C. Fuggle, G.A. Sawatzky, M. Campagna, O. Gunnarsson and K. Schönhammer, Phys. Rev. B30 (1984) 1777.

[6] M. Croft, A. Franciosi, J.H. Weaver and A. Jayaraman, Phys. Rev. B24 (1981) 544.

[7] A. Franciosi, J.H. Weaver, N. Mårtensson and M. Croft, Phys. Rev. B24 (1891) 3651.

[8] E. Wuilloud, B. Delley, W.-D. Schneider and Y. Baer, Phys. Rev. Lett. 53 (1984) 202, 2519.

[9] Y. Baer and Ch. Zürcher, Phys. Rev. Lett. 39 (1977) 956.

[10] J.M. Lawrence, J.W. Allen, S.-J. Oh and I. Lindau, Phys. Rev. B26 (1982) 2362.

[11] J.H. Scofield, J. Electron Spectrosc. 8 (1976) 124.

[12] D.D. Koelling, A.M. Boring and J.H. Wood, Solid State Commun. 47 (1983) 227.

[13] W. Gudat, M. Campagna, R. Rosei, J.H. Weaver, W. Eberhardt, F. Hulliger and E. Kaldis, J. Appl. Phys. 52 (1981) 2113.

[14] T. Satoh, H. Yashima, H. Mori, in: Valence Fluctuations in Solids, eds. L.M. Falicov, W. Hanke and M.B. Maple (North-Holland, Amsterdam, 1981) p. 533.

[15] W.H. Dijkman, A.C. Moleman, E. Kesseler, F.R. de Boer and P.F. de Châtel, in: Valence Instabilities, eds. P. Wachter and H. Boppart (North-Holland, Amsterdam, 1982) p. 515.

[16] E. Wuilloud, W.-D. Schneider, B. Delley, Y. Baer and F. Hulliger, J. Phys. C17 (1984) 4799.

[17] B. Delley and H. Beck, J. Magn. Magn. Mat. 47&48 (1985) 269.

[18] K.R. Bauchspiess, W. Boksch, E. Holland-Moritz, H. Launois, R. Pott and D. Wohlleben, in: Valence Fluctuations in Solids, eds. L.M. Falicov, W. Hanke and M.B. Maple (North-Holland, Amsterdam, 1981) p. 417.

Electron-spectroscopic manifestations of the 4*f* states in light rare-earth solids

W.-D. Schneider, B. Delley, E. Wuilloud, J.-M. Imer, and Y. Baer
Institut de Physique, Université de Neuchâtel, CH-2000 Neuchâtel, Switzerland
(Received 26 June 1985)

The consequences of the degeneracy between configurations with different populations of atomiclike *f* states are studied systematically for a number of light rare-earth materials (Ba, LaF_3, La_2O_3, La, CeO_2, $CeCo_2$, CeN, α-Ce, and γ-Ce) using high-energy spectroscopies. The Anderson impurity model applied to this problem (Gunnarsson-Schönhammer model) is found to describe convincingly a variety of electron-spectroscopic excitations, such as, x-ray photoemission and bremsstrahlung isochromat spectroscopy. We have extended this many-body formalism to account for electron-energy loss spectroscopy and L_{III} absorption edges. The parameters resulting from the calculation are analyzed within the framework of a simplified Hamiltonian containing no coupling terms between *f* and band states. This approach reveals in a natural way the importance of the conventional concept of hybridization. The energy degeneracy and the wave-function overlap of quantum states give rise to a mixing and to a continuous energy distribution of excitations. For electronic transitions described within the sudden approximation the impurity model provides a sound and unified description of the "satellite complex" encountered in the high-energy excitation spectra of such systems.

I. INTRODUCTION

Since the early days of photoelectron spectroscopy, the appearance of satellite lines in core-level spectra has been the subject of many investigations.[1–17] It was recognized that these satellites are closely related to the presence of open 3*d*, 4*f*, and 5*f* shells. Numerous interpretations were given to correlate their intensity and energy positions with the ground-state properties of the solid. For example, in actinide compounds, the appearance of satellite lines in core-level spectra was considered as precursory indication of *f*-electron localization.[12,13] In the rare-earth compounds, the occurrence of two sets of structures in core-level spectra has been interpreted quite often in terms of two localized 4*f* populations.[14] However, in the earliest x-ray photoemission studies of atoms and molecules[1] it was recognized that the sudden potential change resulting from the ionization of a deep core level can induce drastic modifications among the outer electrons: Simultaneous excitations within the outer bound levels can occur or additional weakly bound electrons can be expelled. These two types of processes were called, respectively, electron "shakeup" and electron "shakeoff." Since the main weight of the spectra is usually concentrated on the simple ionization process, the weak structures at larger binding energies corresponding to these additional excitations were considered as satellites. Within the Hartree-Fock approximation and the sudden approximation the necessity of such excitations and the relationship between their distribution and the relaxation energy is rather straightforward.[18] The multiplet splitting resulting from the exchange and electrostatic interactions of incomplete shells will be discarded here. In solids, strong core-level satellites have been first observed in core-level excitations of ionic compounds.[2,3] In an atomiclike model, their origin can be relatively simply explained by a configuration-interaction between distinct final states being close in total energies. At about the same time, a splitting into two components of comparable intensities has been observed in $3d_{3/2,5/2}$ core-level spectra of light rare-earth ionic compounds such as, for example, La_2O_3.[4,5] In the original interpretation, the high-binding-energy peaks were considered as an energy-loss or shakeup process described as a charge transfer from filled ligand orbitals to the empty 4*f* shell after creation of the core hole. A few years later, the observation of three peaks in the core-level spectra of CeO_2 led Burroughs *et al.*[19] to the idea that the presence of a core hole can lower substantially the 4*f* energy relative to the band states, so that the population of a 4*f* state can be the most efficient screening mechanism. For this type of screening transition the terms "energy gain" or "shakedown" satellites have been coined. This picture has been extended by Crecelius *et al.*[20] to the weak 3*d* low-binding-energy satellites observed in the light rare-earth metals.

The first attempts to go beyond an atomiclike description of such satellites in solids have been made by Kotani and Toyozawa[15,16] and Schönhammer and Gunnarsson.[17] They provided a quantitative description in terms of core-hole screening populations originating from coupled states with different symmetries and spatial extents. These approaches represent an important first step toward the more elaborate calculations available today. They are at the origin of the nowadays popular but too schematic expressions "well-screened" and "poorly-screened" final states used for characterizing respectively a low- and a high-binding-energy core line in rare-earth, actinide, and transition elements.[21] At the present time, the accumulation of spectra containing core-level and valence-band satellites demonstrates that this type of manifestation ac-

counts for a rather general situation which is certainly unconventional but not exceptional. Presently the Anderson impurity model appears to provide the simplest framework for describing the excitations of rather localized states which are hybridized with band states. After the first approach of Oh and Doniach,[22] a unified and quantitative many-body calculation scheme for the various core-level and outer-level excitations in Ce has been proposed by Gunnarsson and Schönhammer.[23] Ce with its low $4f$ population offers the simplest conditions for studying this mixing mechanism which has a dominating influence on the spectra and is not involved with complex multiplet structures. The achievements of this model are the following.

(i) A single set of parameters, characterizing the electronic structure of a solid, yields correctly all kinds of excitation spectra. This allows one to reconcile the contradictory pictures of the $4f$ states deduced from the different experimental techniques [x-ray photoemission (XPS), bremsstrahlung isochromat spectroscopy (BIS), electron-energy loss spectroscopy (EELS), x-ray absorption spectroscopy (XAS), susceptibilities, and lattice constants[24–28]].

(ii) The correct width of the bands included into the model allows one to predict the spread and shape of the $4f$ and core spectra in a more realistic way than in any cluster calculation.[29]

(iii) Mixing in initial and final states are taken into account. In both states the $4f$ population is found to be integral only in extreme situations. This invalidates the atomic description and calls in question the use of deep core-level spectroscopy for revealing valence fluctuations.

The aim of this paper is to present and to analyze the electron spectroscopic manifestations of the $4f$ states in a particular sequence of solids where the consequences of f admixture to the band states can be studied in a systematic manner. Despite the hidden aspects of the theoretical computation the behavior of the spectra allows one to understand intuitively how the parameters used to characterize the electronic structure determine the observed excitations.

II. EXPERIMENTAL DETAILS

With the exception of the spectra of La_2O_3 and $CeCo_2$, the data shown and discussed in this work have been taken from already published studies, those of Ba (Refs. 30–33) and LaF_3 (Refs. 7, 34, and 35) as well as of the valence bands of γ-Ce and α-Ce (Ref. 36) have been measured by other authors, those of La (Refs. 37 and 38), CeO_2 (Ref. 39), CeN (Refs. 40–41), α-Ce, and γ-Ce (Ref. 27) originate from the present authors. All our spectra have been obtained in a single instrument which allows us to perform XPS, BIS, and EELS on the same sample without breaking the vacuum of 2×10^{-11} Torr.[42,37]

The La_2O_3 sample was prepared *in situ* from La films freshly evaporated on Cu and oxidized at 300 K in an oxygen atmosphere of 10^{-6} Torr for 6 h. Subsequently the films were exposed for 10 min to an oxygen discharge at 0.1 Torr in order to obtain sufficiently thick La_2O_3 samples. By varying the photon flux or the electron beam current during the different measurements, no charging effect could be detected. The relative position of the energy scales in the XPS and BIS spectra of La_2O_3 were calibrated within 0.1 eV by observing with both techniques the position of the Fermi level (E_F) of a Ag film deposited onto La_2O_3.

The polycrystalline $CeCo_2$ sample was prepared by melting the constituents in a levitation furnace. An x-ray analysis confirmed the Laves phase structure of the compound and no foreign lines due to other phases were detected. Clean surfaces were obtained *in situ* by scraping with an Al_2O_3 file. In order to avoid a rapid surface accumulation of oxygen diffusing from the bulk, the sample was held at liquid-nitrogen temperature.

III. THE MODEL

We have analyzed the XPS, BIS, and EELS spectra within the Gunnarsson-Schönhammer (GS) approach[23] which was originally developed for describing different spectroscopic transitions in metallic Ce compounds. We have adapted this model for L_{III} absorption edges[43] and EELS transitions and we have extended it to insulating rare-earth compounds. In this section we give only a discussion of the model relevant to XPS and BIS. The EELS and L_{III} edges will be treated separately in Secs. VI and VII, respectively. The electronic density of states of insulators was simulated by semielliptical valence and conduction bands separated by a gap. We note, that the large f degeneracy N_f is much less important for insulators than for metals since no low-lying bandlike excitations could lead to divergencies. The calculations have been performed to second order in $1/N_f$ (Ref. 23) and they include basis states up to double f occupation. Lower-order approximations which are useful for Ba metal and La compounds are discussed in the Appendix.

For each compound, the heights, widths, and positions of the bands have been chosen in such a way that the model can account correctly for the mixing of the $4f$ states with the extended states. This schematic band picture represents a weighted density of states (DOS) where the amplitude is proportional to the coupling strength Δ defined in the Appendix. The relevant DOS features are respected, but need not be more realistic since the aim of the model calculation is exclusively the description of the $4f$ contributions to the different excitations. The computed spectra have been compared to all experimental spectra (XPS, BIS, EELS) and the parameters have been varied until the best general agreement is found. In fact, this procedure represents a stringent test of the model. In this way, more reliable parameter values are obtained than by a fit to only one type of experimental spectrum. Among the parameters, the f-f Coulomb repulsion U_{ff} and the Coulomb attraction U_{fc} of the $4f$ states by a core hole are essentially atomic quantities which are renormalized by the screening mechanisms in solids. As shown in Table I, their values do not scatter very much among the different

TABLE I. Relevant energies (eV) and populations obtained from the fit of the many-body calculations to the experimental spectra.

Material	Δ_{fp}	Δ_{fd}	ϵ_f	U_{ff}	U_{fc}	n_f
Ba		0.1	14.0	8	−12	0.003
LaF_3	0.6	0.06	14.5	8	−13.5	0.002
La_2O_3	0.6	0.06	10.7	8	−12	0.04
La		0.08	5.5	8	−9	0.01
CeO_2	0.6	0.06	0.5	8	−12	0.45
$CeCo_2$		0.3	−1.2	5.5	−10	0.76
CeN	0.2	0.1	−0.8	7	−11	0.80
α-Ce		0.08	−1.2	6	−10	0.88
γ-Ce		0.03	−1.5	6	−10	0.98

types of solids considered. Only two parameters remain completely free in the fitting procedure: the hybridization energy Δ defined in the Appendix, and ϵ_f representing in the limit of $\Delta=0$ and $U_{ff}=0$, the energy difference between consecutive f counts. The values of the initial $4f$ populations n_f, also given in Table I have not been adjusted but they are a result of the model calculation.

Once all these parameters are known from the model calculation, it is very instructive to take a step backwards and to discuss the results within the framework of a simplified Anderson impurity Hamiltonian without the hopping term:

$$H_u=\sum_k \epsilon_k n_k+\epsilon_f \sum_m n_m+U_{ff}\sum_{m'>m} n_{m'}n_m$$
$$+n_c\epsilon_c+(1-n_c)U_{fc}\sum_m n_m \ .$$

The orbital indices m and k for the $4f$ and valence states implicitly include the spin. We note that the parameters entering the uncoupled Hamiltonian H_u can be estimated in principle from a parameter free density-functional calculation.[44] For the discussion of excitation spectra it is convenient to choose as an origin of the total-energy scale the total electronic energy of the ground-state configuration (this definition remains valid for the model calculation). In this simple scheme the population changes induced in the bands, $4f$ levels or core levels, are assumed to be screened by charge transfer among the highest occupied band states. This mechanism corresponds to a negligible variation of the Fermi-energy position in a metal and it supposes the creation of a polarization charge originating from the valence-band top in an insulator. This assumption appears to provide the correct way to relate on a total-energy scale the single-particle excitations of extended states to the total energies involved in population variations of highly correlated states. Within this simple framework ($\Delta=0$), the density of the single-particle excitations of the outer levels, relevant for these spectroscopies, will be called "uncoupled $S(E_t)$." This quantity is composed of the weighted density of states discussed previously and of the discrete spectrum for uncoupled f states. As shown in Fig. 1 this uncoupled $S(E_t)$ can be split into electron-addition and electron-subtraction processes which must be represented on a common total-energy scale in order to be consistent with the Hamiltonian. It is more usual to represent these two types of excitations within a single-particle excitation spectrum where the states are given as a function of the energy of one electron occupying the considered level. This representation is just obtained from the previous one by a 180° rotation

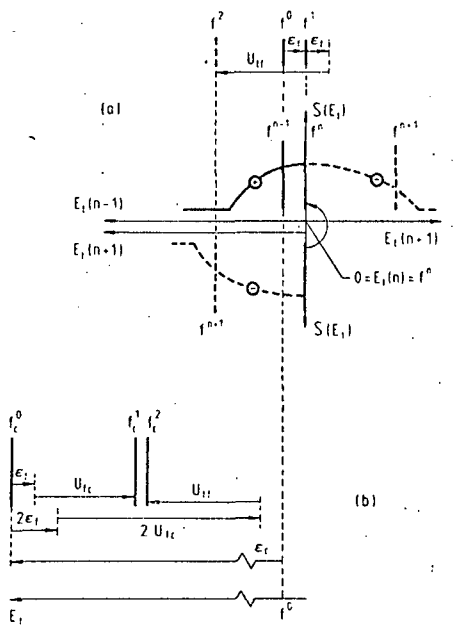

FIG. 1. (a) Screened single-particle excitations of the extended and localized outer levels without coupling as a function of the total electronic energy E_t of the final state: uncoupled $S(E_t)$. *Left part*: uncoupled $S(E_t)$ resulting from the addition (thick dashed lines) and subtraction (solid lines) of one electron represented separately on a common total-energy scale. The position of f^n represents the total energy of the ground state and does not belong to the excitation spectrum. The parameters linking the different $4f$ populations shown in the top of the figure are correct only for an uncoupled $4f^1$ ground state. *Right part*: the uncoupled $S(E_t)$ for electron addition rotated by 180° around the origin in order to make it consistent with the usual single-particle representation of the excitation spectra (XPS + BIS). (b) Lowest total energies of the different uncoupled final states in the presence of a core hole for an f^1 ground state. This diagram is most conveniently constructed by starting from the total energy of an initial $4f^0$ configuration. The creation of a core hole raises this energy by ϵ_c. In addition to the other parameters one has now to take into account the core-hole attraction U_{fc}. The relative positions of the different final-state populations can be easily calculated from the simplified Hamiltonian.

of the electron-addition spectrum. For two atoms in an uncoupled ($\Delta=0$) $4f^n$ ground-state configuration one can verify in the single-particle or total-energy representation that U_{ff} corresponds to the common definition of the Coulomb correlation energy involved in the formation of the two noninteracting polar states $4f^{n-1}$ and $4f^{n+1}$. When only f states are considered, one has to realize that their energy is given by

$$E_n(f^n)=n\epsilon_f+\tfrac{1}{2}n(n-1)U_{ff} .$$

This is just the parabolic behavior of the total energy as a function of the f population.

When the hopping terms accounting for the overlap in space of the $4f$ and band states are included, a hybridization can take place between these two kinds of states when they are not too far from the degeneracy. This mechanism becomes particularly important when the total energy of a neighbor configuration (f^{n+1} or f^{n-1}) approaches the total energy of f^n; ground states are formed with fractional f counts which can be very different from integral numbers. The virtue of the GS model is to provide a scheme for the calculation of these states and for the different excitation spectra within the sudden approximation. The complication of this hybridization problem originates from the energy spread of the band states and from the f degeneracy.

For the description of core-hole excitations it is convenient (but not absolutely necessary) to start from the total energy of the initial configuration f^0 even if it is not the ground-state configuration. In the presence of a core hole ($n_c=0$), this energy is simply raised by ϵ_c as shown in Fig. 1(b). In the uncoupled scheme, it is then a simple matter to calculate the relative positions of the other final-state f populations by inserting the suitable numbers (Table I) in the simplified Hamiltonian. The simultaneous excitations of band states created in the core-hole ionization should be represented in Fig. 1(b) as continua extending from each f^n level toward higher total energies. For this reason the measured and computed excitation spectra show in some cases more complicated or extended structures than expected from the mixing of the narrow uncoupled states. As long as the different accessible f^n final states are well separated and/or the hybridization parameter Δ remains negligible, the position of the peaks in the core-level spectra are well predicted by the uncoupled energies. The intensity of each peak accounting for a practically integral f population reflects the strength of these configurations in the initial states.

An important final-state mixing can only occur when, simultaneously, the value of Δ is sizable and two uncoupled configurations with different f counts have nearly or completely degenerate total energies. Furthermore, the coupling is strong only if their f-population difference is one electron. In this case, split levels are formed by hybridization, each of them containing comparable contributions from the two uncoupled states. The weight of the two configurations forming the mixed states is no longer representative of the initial ground state. In such extreme situations, it makes no sense to attempt any identification of the two observed peaks in terms of different integral $4f$ populations and to interpret their ratio as the mixing of the initial state. A discussion about the energy separation between these hybridized peaks is given in the Appendix. Finally, one should notice that the multiplet splitting has not been included in these calculations.

IV. SYSTEMS WITH $4f^0$ GROUND-STATE CONFIGURATION IN THE UNCOUPLED SCHEME

The systems selected and discussed in this section have in common the fact that in the uncoupled scheme ($\Delta=0$) the total energy is larger in the $4f^1$ configuration than in the $4f^0$ configuration ($\epsilon_f>0$). This means that without hybridization they would all be in a pure $4f^0$ ground state. In Fig. 2 these systems have been disposed vertically in a sequence where the energy difference ϵ_f decreases gradually. We shall consider at first the outer-level excitation spectra which are shown in Fig. 2(a) together with the corresponding uncoupled $S(E_t)$ and the model calculations. Except for CeO_2, discussed separately later, the influence of the hybridization remains negligible in the direct population changes induced in XPS and BIS. This is an obvious consequence of the large energy separating the $4f^0$ and $4f^1$ configurations. Even in LaF_3 and La_2O_3, where large values of Δ are obtained, the initial $4f^1$ population n_f is well below 0.1 and in the model calculation of the photoemission spectra its contribution can be barely discerned. Therefore, the structures observed in the XPS spectra must be interpreted as band excitations. The $4f$ contributions to the BIS spectra have been shaded in order to distinguish them from the population of extended states. Besides strong variations of the width, attributable to the lifetime broadening and to the different instrumental resolutions, the model calculation traces the f contributions of the BIS spectra very well. In these systems, with the exception of CeO_2, the model calculation for the outer-level excitations is not necessary, since it reproduces faithfully the energy positions of the uncoupled $4f^1$ states.

The situation becomes more interesting in CeO_2, where the uncoupled f^0 and f^1 energies are very close. This proximity and the large value of Δ give rise to a sizable mixing of f^1 with f^0 states responsible for the important initial $4f$ population $n_f\sim0.5$. The fact that CeO_2 is an insulator constrains this ground-state mixing to occur within the full valence band, which must accommodate this f admixture of extended nature. This contribution does not exhaust all the available $4f^1$ states so that another type of $4f^1$ states is found at higher single-particle energies, in the range where the population of extended states is forbidden (band gap of the extended states). For this reason the admixture remains small in the gap where nearly pure $4f^1$ states are formed. The agreement of this description resulting from the impurity calculation with a band calculation is gratifying.[45] The weak $4f^1$ admixture to the valence band cannot be distinguished in the total XPS spectrum. The BIS spectrum is dominated by the $4f^1$ peak, whereas the broad $4f^2$ final states mixed with conduction-band states, are embedded into the signal originating from extended states and the background. There have been controversies in the literature whether compounds like CeO_2 should be called mixed valent or not.[46,47,29] According to Varma,[48] the term mixed valent

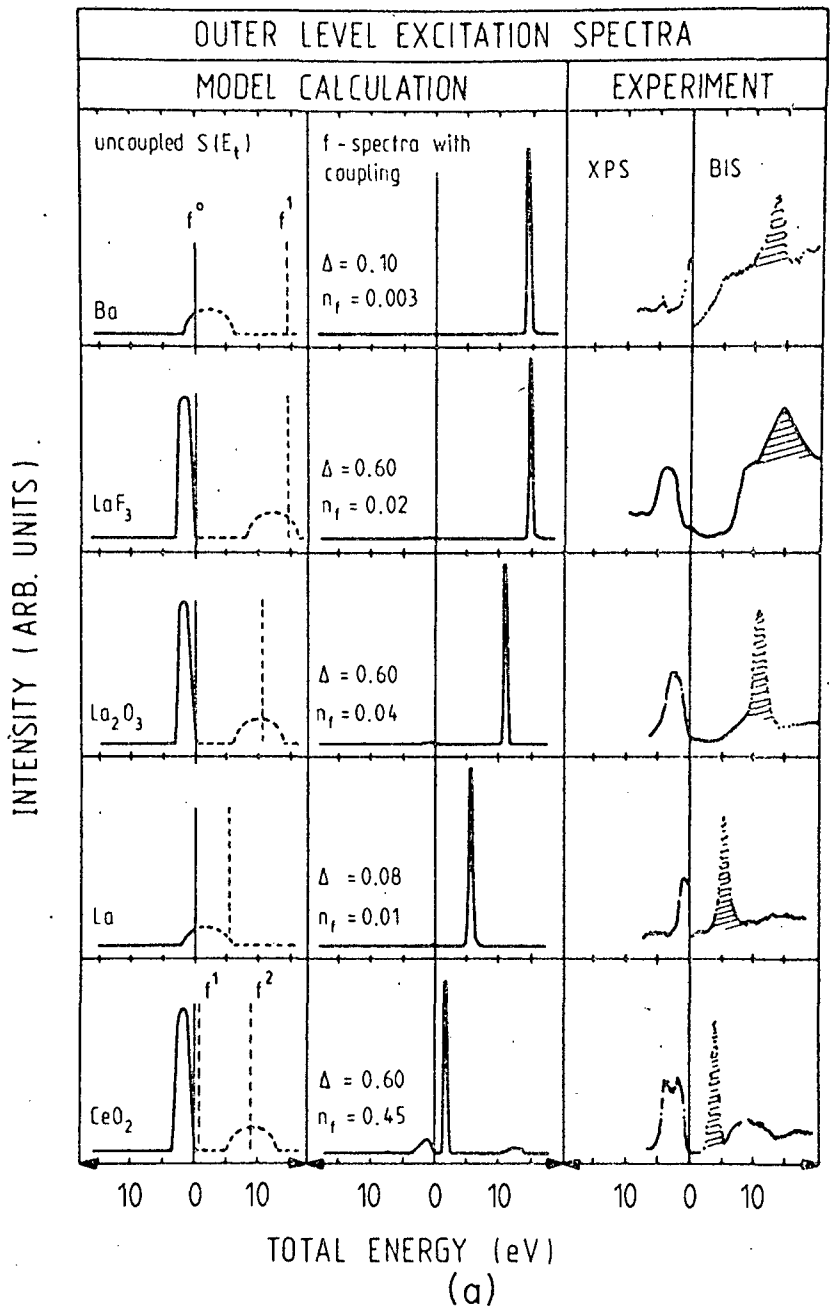

FIG. 2. (a) Calculated and measured outer-level excitation spectra. In the uncoupled $S(E_f)$ (see Sec. III), the amplitude of the valence and conduction bands is chosen proportional to the hybridization parameter Δ. In the calculation of the f spectra with coupling, a Gaussian instrumental broadening of 0.4 eV full width at half maximum (FWHM) has been included. The experimental spectra have been taken from the following works. XPS: Ba (Ref. 30); LaF_3 (Ref. 34); La_2O_3, La (this work); CeO_2 (Ref. 39). BIS: Ba (Ref. 32); LaF_3 (Ref. 35); La_2O_3, La (this work); CeO_2 (Ref. 39). The origin of the total-energy scale is the Fermi energy in metals and the upper valence-band edge in insulators. The f contribution corresponds to the hatched areas. (b) Calculated and measured $3d$ core-excitation spectra (see Sec. III). In the spectra with coupling the solid curves correspond to XPS and the dotted curve to EELS. The calculated spectra have been convoluted by a Lorentzian of 1.2 eV FWHM to include lifetime broadening. The experimental spectra have been taken from the following works. XPS: Ba (Ref. 30); LaF_3 (Ref. 7); La_2O_3, La (this work); CeO_2 (Ref. 39). EELS: Ba (Ref. 33); CeO_2 (Ref. 39). The XPS and EELS spectra have a common energy scale and the centers of gravity of the EELS final states are indicated by arrows in the corresponding XPS and EELS spectra.

characterizes the fractional occupation of localized states in metals. This is obviously not the case in CeO_2 where the Ce atoms are tetravalent, since no atomiclike localized f level is occupied and the four outer electrons are involved in the covalent p-d and p-f admixture to the chemical bond.

The XPS $3d$ core-level excitations displayed in Fig. 2(b) contain many unconventional aspects, which can be easily understood by considering the initial-state situation described previously and the uncoupled final-state positions obtained [Fig. 1(b)] with the parameters given in Table I. (The discussion of EELS spectra is delayed to Sec. VI.) From Ba to La, the initial-state mixing is negligible and the ground-state configuration is nearly pure

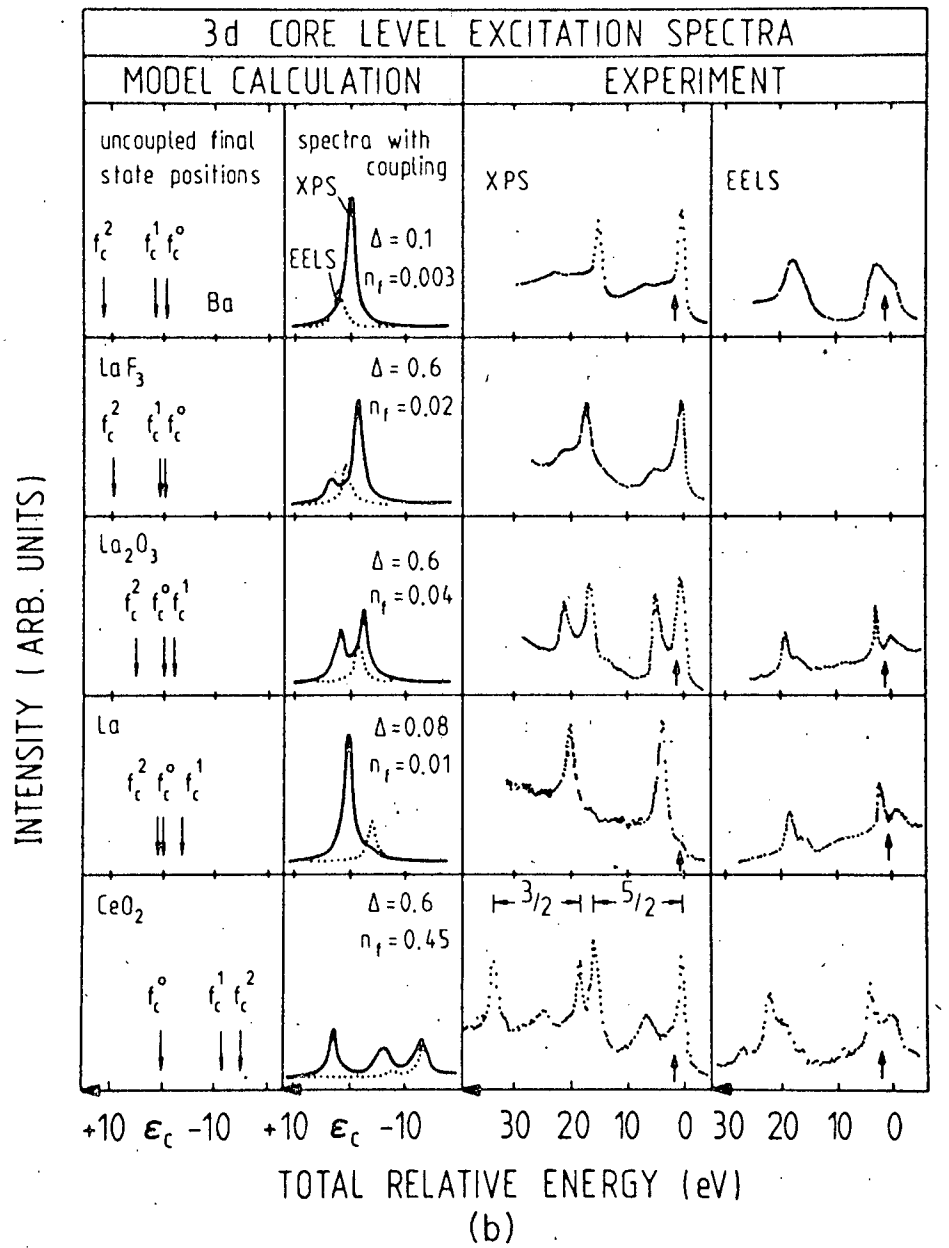

FIG. 2. (*Continued*).

$4f^0$. The presence of a core hole decreases dramatically the total-energy difference between the $4f^1$ and $4f^0$ configurations so that a final-state mixing becomes possible. In Ba metal the value of Δ is still too small to induce a detectable hybridization and the model predicts a simple Lorentzian line shape. The XPS $3d$ lines confirm this expectation since the pronounced asymmetry is due to electron-hole pair excitations not included in the model and the small satellite can be identified with a plasmon excitation.[49] In the insulator LaF_3, the value of the hybridization parameter Δ is now 0.6 eV and the resulting final-state mixing is responsible for the two peaks predicted and observed in the $3d$ core-level spectrum. In this case an identification of the two structures with different integral $4f$ populations is dubious and only the more intense one has a clearly dominant $4f^0$ component. In La_2O_3, the order of the f_c^1 and f_c^0 final-state positions is inverted and the value of Δ is large again. The consequence is a splitting of the core-hole final state into two components of nearly equal intensities.[4,6,7,19,21,11] Each of them is formed by a mixing of the two configurations f_c^0 and f_c^1 in a ratio of approximately one to one and their separation is mainly determined by Δ (see Appendix). Furthermore, the analysis of the model calculation shows that in fact the excitation spectrum does not consist simply of two neighbor peaks, but corresponds to a continuous intensity distribution reflecting excitations of valence states through the whole bandwidth. La_2O_3 provides one typical example that demonstrates that the traditional interpretation of each peak in terms of pure atomic configurations is completely in error.

At this point it is interesting to consider briefly the evolution of the different excitation spectra of the trivalent-La compounds with F, O, Cl, and Br.[6,7] The decrease of

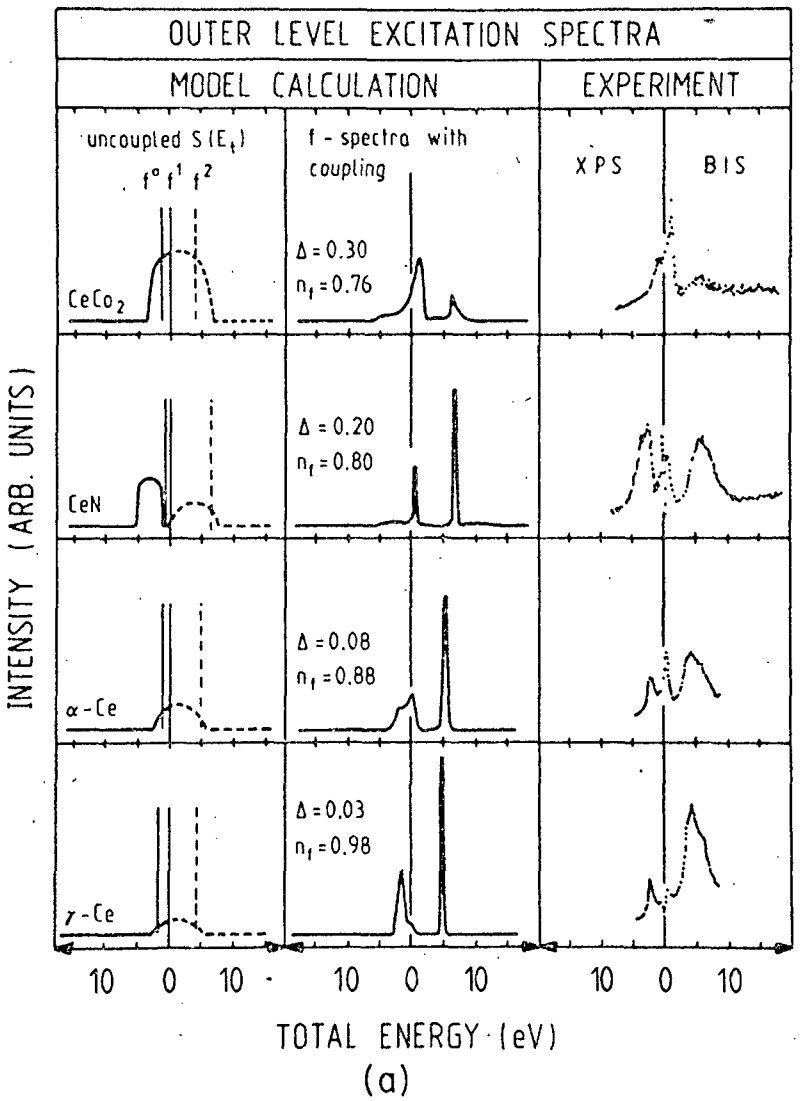

FIG. 3. (a) Calculated and measured outer-level excitation spectra [see caption of Fig. 2(a)]. The experimental results originate from XPS: $CeCo_2$ (this work), CeN (Ref. 41), α- and γ-Ce (Ref. 36); BIS: $CeCo_2$ (this work), CeN (Ref. 41), α- and γ-Ce (Ref. 27). (b) Calculated and measured $3d$ core-excitation spectra [see caption of Fig. 2(b)]. The experimental results originate from XPS: $CeCo_2$ (this work), CeN (Ref. 40), α- and γ-Ce (Ref. 27). EELS: $CeCo_2$ (this work), CeN (Ref. 41), α- and γ-Ce (Ref. 27).

electronegativity in this sequence[50] corresponds to an increase of the charge available for the screening around the La atom. This strengthening of the screening power with decreasing ligand electronegativity contributes certainly to the reduction of the total energy involved in the creation of core holes (chemical shifts). The same mechanism is assumed to be responsible for the important decrease of the $4f^1$ total energies observed in the BIS spectra of Fig. 2(a) for the sequence LaF_3, La_2O_3, La metal. Such shifts in inverse photoemission of localized levels are at variance with the conventional interpretation of the chemical shift based only on simple electrostatic considerations in the initial state. Proceeding now from La_2O_3 to $LaCl_3$ and $LaBr_3$, one can anticipate that the energy difference between f_c^0 and f_c^1 is still increasing. Assuming a constant Δ, the model calculation for this evolution of the uncoupled final-state energies shows that the intensity is transferred from the low-energy peak LaF_3 to the high-energy peak $LaBr_3$, in perfect agreement with the measurements.[6,7] It is important to notice that in both extreme situations where the mixing is not too strong, the most intense peak has a dominant f^0 character reflecting the initial-state configuration. The model calculation appears to provide a sound and unified description of the La "satellites" which have given rise to so many intuitive interpretations.[4,6,11,19,21]

In La metal, f_c^0 and f_c^1 energies are not quite as close and Δ is small. Since the initial $4f^1$ population is negligible ($n_f = 0.01$) and the conditions for a final-state mixing are not favorable, the excitation spectrum contains essentially a leading f_c^0 peak accompanied by a weak f_c^1 satellite. In this case, nearly pure final-state configurations are realized. It is interesting to notice that from the f^0 initial state, the matrix element expressing the sudden approximation for a core-electron photoemission provides practically no intensity to the f_c^2 final state. Despite the fact that the two configurations f_c^2 and f_c^0 are nearly degenerate, the effective hybridization between states with f-

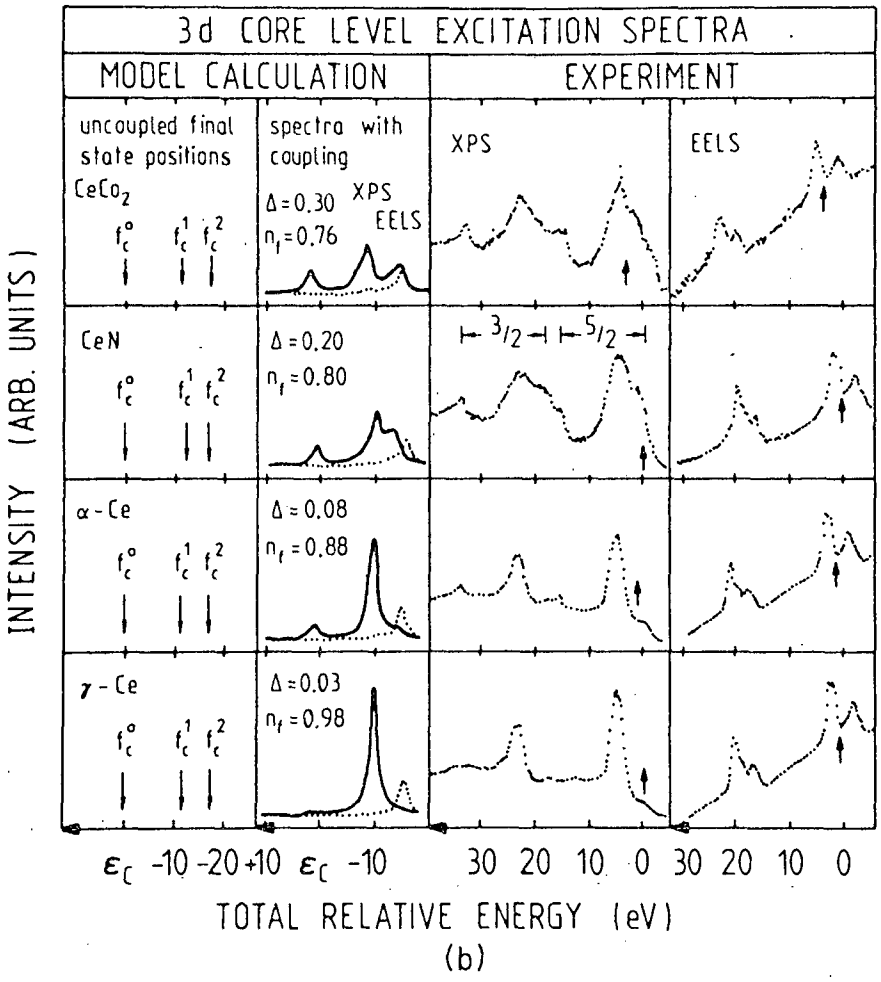

FIG. 3. (*Continued*).

count differences larger than one is negligible.

Finally, in CeO_2 the relative positions of the uncoupled energies of the different f^n configurations are drastically modified when a core hole is created. f_c^0 has now the highest energy and is well separated from f_c^1 and f_c^2. For this reason it cannot hybridize and consequently appears as a simple isolated peak with a large intensity accounting for the important f^0 character of the initial state. The two close f_c^1 and f_c^2 configurations together with band excitations form a strongly mixed final-state continuum dominated by two leading peaks. The observation of a large intensity for states of this nature is a consequence of the existence of the $4f^1$ initial population of extended states which is in this way indirectly demonstrated. For all these $3d$ core-level spectra, the agreement between the model calculation and each spin-orbit-split component of the XPS spectra is striking and requires no further comment.

V. SYSTEMS WITH $4f^1$ GROUND-STATE CONFIGURATION IN THE UNCOUPLED SCHEME

In Figs. 3(a) and 3(b) the outer and core-level excitation spectra for $CeCo_2$, CeN, α-Ce, and γ-Ce are presented, respectively. They have been selected and displayed vertically according to increasing f occupation n_f in the ground state. The common property of these materials is the $4f^1$ configuration of their uncoupled ground state, obtained from the best fit of the model calculation to the experimental spectra, as shown in Fig. 3(a). For these materials the total energy is larger in both the $4f^0$ (electron-subtraction) and in the $4f^2$ (electron-addition) configuration). The uncoupled f^0 and f^1 total-energy positions are not far from degeneracy allowing for a mixing of these two configurations when the coupling strength Δ becomes sizable. For these conditions the model calculation yields the peculiar excitation spectra displayed in the second column of Fig. 3(a). The BIS excitations show essentially two peaks corresponding roughly to the energy positions of the f^1 and f^2 configurations in the uncoupled $S(E_t)$. On the other hand, the XPS excitations are a mixture of f^0 and f^1 configurations producing a continuum of states with a characteristic two-peak intensity distribution. This spread of f intensity over the whole bandwidth is particularly evident for $CeCo_2$ and α-Ce where it reflects the more covalent character of the f charge. We note that this interpretation is fully consistent with the results from ground-state band calculations.[51]

With decreasing coupling strength Δ or/and increasing total-energy separation between f^0 and f^1 configurations, the outer-level excitation spectra tend to become similar to the ones known for the localized f states in heavy rare-earth materials. in γ-Ce most of the spectral weight is

found at the uncoupled f^0 and f^2 energy positions and the ground-state f occupation n_f approaches unity. It is also evident from the calculated spectra that the increase of n_f is correlated with a decrease in total energy for the $4f^2$ excitation.

For a comparison between theory and experiment only the area of the corresponding $4f$ signals must be considered, since multiplet splitting has not been included in the many-body calculation. For $CeCo_2$ (Ref. 52) and CeN the emission from Co d states and N p states must not be confused with f emission. Generally good agreement between calculated and measured spectra is obtained for the BIS excitations which show above the $4f^1$ peak the typical structure corresponding to the population of the $4f^2$ multiplets. Moreover, the predicted weight transfer from f^1 to f^2 final states is confirmed in the sequence $CeCo_2$ to γ-Ce. In the XPS spectra of $CeCo_2$ and CeN the small cross-section ratio between f and valence states impedes the observation of the $4f$ contribution in the region of the other band electrons. For α-Ce and γ-Ce, however, the data are taken from resonant photoemission work[36] where the enhancement of the f contribution allows an easier comparison with the model. In this case the overall agreement between experiment and calculation is satisfactory, especially the predicted decrease of the ratio between the f intensity at the Fermi level, and at ~ 2 eV is noticeable in the data.

The rather unique case of the metallic compound CeN deserves special interest.[41] The uncoupled $S(E_f)$, with a p valence band separated by a small gap from the d conduction band, exhibits a close similarity with the electronic structure of the insulator CeO_2. However, in contrast to CeO_2, only three electrons of Ce are necessary to complete the p band of N in CeN. For this reason the p-f mixing remains small, despite the rather important coupling parameter $\Delta_{fp}=0.2$ eV and the small energy difference between f^1 and f^0. This situation is reflected in the spectra by the fact that very little f intensity is spread over the p band. On the other hand, the remaining f electron plays an important role in the formation of the metallic state in CeN. In the uncoupled scheme the f^1 total energy is about at the bottom of the d band so that the coupling $\Delta_{fd}=0.1$ eV is responsible for the metallic state of this compound. The calculation yields a fractional f occupation $n_f=0.8$ in the ground state. This description is dictated by the choice of parameters producing the best agreement of the many-body calculation with the $4f$ and core excitations (see below). A recent ground-state band calculation is also compatible with this description of the extended states.[53] The moderate value of Δ_{fp}, the very small f^0-f^1 energy difference and the fact that a single electron is involved in the hopping mechanism $f^0d^1 \leftrightarrow f^1d^0$ seems to provide in CeN the most favorable conditions for the mixing mechanism called valence fluctuation.

Finally, we have to mention that an *ab initio* supercell band-structure calculation for the outer-level excitations in Ce and Ce compounds[54] is in qualitative agreement with the electronic states description obtained in the present analysis of the experimental spectra. CeN is also found to have a peculiar behavior. It is interesting to note that an f occupancy of ~ 0.8 is obtained for CeN, in quantitative agreement with the present calculation.

The creation of a core hole in these materials raises the total energy of the initial $4f^0$ state by ϵ_c. Then, according to Fig. 1(b) and Table I, the interactions U_{fc} and U_{ff} lead to the uncoupled final-state positions of the relevant $4f$ configurations displayed in Fig. 3(b). The uncoupled f_c^1 and f_c^2 final states are not too far from degeneracy, while the $4f_c^0$ state remains well separated from them. The situation in the presence of a core hole is thus markedly different from the one without a core hole, where the f^0 and f^1 configurations are nearly degenerate and the f^2 state has a considerably higher total energy [cf. Fig. 3(a)]. If now the hybridization is taken into account, the interaction with the band continua allows the mixing of the f_c^1 and f_c^2 configurations in the final state, giving rise to the calculated excitation spectra, shown in column 2 of Fig. 3(b). For an important coupling, like in $CeCo_2$ and CeN, this mixing between f_c^1 and f_c^2 final states is strong in each of the two peaks around 10 eV below ϵ_c. With decreasing hybridization, the intensity of the structure at the lowest total energy decreases, allowing in α-Ce and γ-Ce for a traditional identification of the two structures in terms of $4f_c^1$ and $4f_c^2$ final-state populations. On the other hand, as a consequence of the large energy separation, the f_c^0 final state at ϵ_c remains essentially pure even for the strong coupling occurring in CeN and $CeCo_2$ and their intensity evolution reflects rather well the f^0 populations $(1-n_f)$ of the different ground states.[23]

At first sight, the comparison between calculated and measured XPS $3d$ core-level spectra may appear to be rather difficult since the $3d_{5/2}$-$3d_{3/2}$ spin-orbit components overlap partially in the middle of the spectra. However, the n_f-dependent intensity of the structures corresponding to the uncoupled f_c^0 final state is most clearly seen in the $3d_{3/2}$ component at high total energies, whereas the Δ-dependent changes in the two-peak structure, corresponding to the mixing of the uncoupled f_c^1 and f_c^2 final states, can be easily observed in the $3d_{5/2}$ component at low total energies. The comparison reveals a remarkable correspondence between calculated and observed spectral shape for CeN, α-Ce, and γ-Ce. For $CeCo_2$ the structures predicted by the calculation below ϵ_c seem to be washed out in the experimental spectrum. This effect is most probably due to the multiplet splitting which is not included in the model calculation or to lifetime broadening.

The outer- and core-level excitations for these materials with uncoupled $4f^1$ ground-state configurations are very well described by the GS model. Two conditions for the observation of unconventional excitation spectra are encountered: two configurations are nearly degenerate and a sizable coupling of the f states with the band states occurs. We want to point out once more that the two configurations f^1 and f^2 which have well-separated total energies do not mix at moderate hybridization in the outer-level excitations but they may do so in the presence of a core hole. Consequently, the intensities of the two structures resulting from their mixing in core-level spectra are by no means representative of f^1 and f^2 ground-state populations.

VI. EELS VERSUS XPS CORE-LEVEL SPECTRA

The use of the electron-energy loss spectroscopy (EELS) as a core-level spectroscopy requires a sufficiently high primary energy (1500 eV) in order to observe and analyze the electrons escaping the sample after having ionized a core level. We present in Figs. 2(b) and 3(b) the losses corresponding to the transitions from the $3d$ shell to the first unoccupied levels. In contrast to XAS processes, the EELS processes are not submitted to strict selection rules, only for primary energies much larger than the energy of the transition and at very small momentum transfer, the dipole selection rules are approximately obeyed. However, in the intermediate-energy range, it is established that the $3d \rightarrow 5d$ single-particle matrix elements are negligible when compared to those determining the intensity of the $3d \rightarrow 4f$ transitions. For this reason within the sudden approximation, the EELS many-body matrix element contains only a creation operator for an f state. This is quite different from the XPS transitions where a high-energy free electron is created. The important consequences of this difference in the core-level spectra can be easily understood schematically by considering the two types of transitions within the simplified framework of the Hamiltonian without hopping terms (see Sec. III). The mixing between two configurations is made artificially impossible so that an f^n initial state is projected only on an f_c^n final state in XPS and only on an f_c^{n+1} final state in EELS. The introduction of the coupling terms does not change very much from this situation for EELS processes where the initial configuration has a nearly integral population f^n: in the final state, the excited electron is forced to occupy an f orbital so that usually the best screened state f_c^{n+1} is naturally formed. On the other hand, for fractional f occupations, final-state mixing will necessarily take place in EELS. The situation is quite different for XPS processes where the frozen initial configuration has no longer the lowest available total energy in the presence of a core hole (except for Ba and LaF_3). In this case, different final states must be realized in order to produce the correct mean energy required by the sudden approximation.

The EELS spectra referenced to the primary energy of the beam provide a straightforward measure of the energy involved in the transitions. For technical reasons it is not possible to obtain absolute transition energies directly from XPS core-level spectra. However, with the assumption proposed in Sec. III concerning the location of the screening charge among the outer states, a common total-energy scale for XPS and EELS is simply obtained by a calibration. In fact, the same assumptions are used in the model calculation in order to represent on a common energy scale the computed XPS (solid line) and EELS (dotted line) spectra [Figs. 2(b) and 3(b)]. The multiplet splitting, particularly important in EELS,[55,56,37] has not been incorporated into the calculation. In order to make the comparison easier, the centers of gravity of the EELS final states have been calculated and their positions are indicated by arrows in the corresponding XPS and EELS spectra.

The agreement between calculated and measured relative energy positions in XPS and EELS is striking. Therefore we refrain from a detailed discussion of the spectra and comment only on a few points of specific interest. It is particularly satisfying to observe that the calculated crossing of f_c^1 and f_c^0 uncoupled positions in the sequence Ba, La_2O_3, La is fully confirmed by the experiment. The fact that the EELS final-state position in La_2O_3 is near the center of gravity of the XPS excitations proves directly the different character of the corresponding final states. It verifies experimentally the validity of the sudden approximation requiring for this particular case of a nearly pure f^0 initial state that the mean final-state energies observed in XPS and EELS spectra correspond approximately to the positions of the uncoupled configurations f_c^0 and f_c^1, respectively.

A weak satellite present in the calculated spectra for fractional occupation in EELS is also clearly visible in CeO_2 and (less prominent) in $CeCo_2$. In addition, the observed EELS structures for these systems differ from the characteristic multiplets corresponding to nearly integral f^1 or f^2 final-state populations.[56,37,57] These facts reflect the consequences of the initial-state mixing in the final state. However, in order to analyze this mixing in detail for the experimental EELS spectra, a many-body theory including multiplet splitting is needed.

VII. $L_{II,III}$ ABSORPTION EDGES VERSUS XPS CORE LEVELS

The $2p \rightarrow 5d$ photoabsorption processes involved in $L_{II,III}$ absorption edges can be considered as identical in first approximation to those occurring in the XPS ionization of any deep core level. The dipole selection rules offer to the excited electron only the possibility to occupy an extended ϵd band state. The basic Hamiltonian does not include Coulomb correlation energies between band electrons and the localized electrons, the core and f electrons. No hybridization between core and band electrons is included and coupling between f and ϵd electrons is forbidden by symmetry. The quantity $W^2(\epsilon)$ includes the dipole matrix element for absorption and the single-particle density of states. For the present calculations we have ignored the details of the energy dependence of W^2 and assumed a smooth form: $W^2(\epsilon)=\sqrt{\epsilon}\, e^{-\epsilon/\lambda}$, where λ is an adjustable parameter. As our Hamiltonian does not provide a coupling between the outgoing ϵd electron and the remaining electronic system, the excitation process is the same as the one for XPS core spectroscopy. The analogy with a XPS process becomes obvious: for one particular transition the sudden approximation matrix element is identical to the one for the XPS transition which involves the energy $\hbar\omega-\epsilon$ and has the spectral weight $\rho_c^{\mathrm{XPS}}(\hbar\omega-\epsilon)$. This last quantity is precisely the intensity of the $3d$ core-level spectra computed with the model calculation and shown in Figs. 2(b) and 3(b). Within this simple Hamiltonian, the total absorption at the photon energy $\hbar\omega$ is given by the following convolution:

$$\rho_{p\rightarrow d}^{\mathrm{XAS}}(\hbar\omega)=\int d\epsilon\, W^2(\epsilon)\rho_c^{\mathrm{XPS}}(\hbar\omega-\epsilon)\,.$$

In order to define the XAS spectra on the common energy scale of the other core-level spectroscopies, it has to be

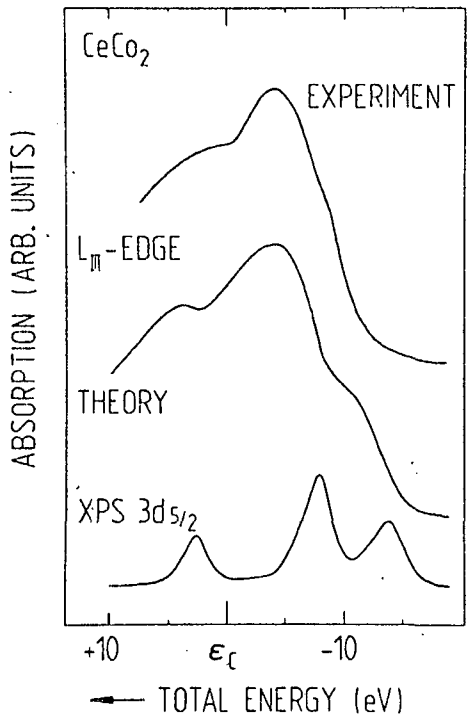

FIG. 4. Calculated and measured L_{III} absorption edge for $CeCo_2$. The calculated edge is obtained by convolution of the XPS $3d_{5/2}$ core spectrum with the function $W^2(\epsilon)=\sqrt{\epsilon}e^{-\epsilon/\lambda}$ (see Sec. VII). The experimental spectrum was taken from Ref. 58.

represented as a function of $\hbar\omega-\epsilon_c$. This expression obtained for the $L_{II,III}$ edges is nothing else than a XPS core-level spectrum washed out by the convolution with the function $W^2(\epsilon)$.

Figure 4 shows a comparison between the measured[58] and calculated L_{III} edge of $CeCo_2$. The model calculation of the $3d$ XPS core-level spectrum presented in Fig. 3(b) and the function $W^2(\epsilon)$ with $\lambda=7$ eV have been used for this computation. The three distinct peaks in the XPS spectrum can be recognized as attenuated and broadened structures in the L-edge spectrum. In view of the approximations made in the model, the overall agreement in position and intensities between the calculated and measured spectral features is surprisingly good. Similar comparisons attempted for La_2O_3, CeO_2, α-Ce, and γ-Ce are less satisfactory but they still confirm that this model is a correct first approximation. Obviously the real form of $W^2(\epsilon)$ and other possible interactions of the excited electrons with the outer electrons of the solid need to be taken into account.

Quite often in such systems, the $L_{II,III}$ edges have been analyzed as if they were formed of overlapping Lorentzian lines and their intensity ratios were considered to reflect directly the configuration mixing in the initial state. This analysis has been promoted as an accurate standard technique for determining the valence.[59–65] Within the formalism proposed in the present paper, it is not possible to find any sound foundation for such an analysis and to attribute any physical meaning to the valence determined in this way.

VIII. CONCLUSION

The light rare-earth solids offer a unique possibility to investigate the different spectroscopic manifestations resulting from the coupling of an atomiclike $4f$ state with extended band states. In order to avoid complicated multiplet effects, the present study has been limited to the elements Ba, La, and Ce which contain at most one occupied $4f$ state. The orbit of these $4f$ states has just the critical dimension to give rise to a sizable mixing with wave functions of neighbor atoms but the resulting hybridized states can hardly be classified either as localized or extended. For this reason, the excitation spectra of these systems show many unconventional aspects which can be explained neither within the atomiclike model nor within the bandlike model which are commonly used in clear-cut situations. At the present time, the Anderson impurity model appears to provide the simplest framework containing the essential aspects of this problem. The success of this model applied to the calculation of the different spectroscopic excitations (Gunnarsson-Schönhammer model) settles its validity for describing the $4f$ and core-level spectra when they are observed with the usual resolution (0.1–0.5 eV) currently achieved in experiments. The apparently hidden aspects of the full many-body calculations can be easily deciphered when the meaning and the interplay of the different parameters defined in the Anderson Hamiltonian are discussed in a conventional description. Without coupling terms, this Hamiltonian provides a schematic location of the initial and final states on a total-energy scale. This approach offers an easy way to recognize the critical situations where the energy degeneracy of configurations with different f counts, together with a non-negligible wave function overlap of f states with band states (sizable Δ), give rise to a strong hybridization. Surprisingly, it took a very long time to realize that this conventional concept of hybridization, already invoked in the early photoemission studies of satellites, provides the simplest suitable framework for interpreting high-energy excitations in rare-earth solids. The challenge is now to refine the many-body theory and to improve the experimental resolution in order to elucidate the mechanisms giving rise to the valence fluctuation and heavy-fermion manifestations.

ACKNOWLEDGMENTS

The authors would like to thank H. R. Moser for taking preliminary data on La_2O_3 and express their gratitude to S. Hüfner who provided the XPS spectra for Ba metal prior to publication. H. Beck is gratefully acknowledged for stimulating discussions. The financial support from the Swiss National Science Foundation is highly appreciated.

APPENDIX

Some details of a lowest-order theory are presented here. A rectangular band is assumed and f^1 admixture in the ground state is neglected. This approximation to the higher-order theory used for the calculation of the excitation spectra shown in Figs. 2 and 3, is sufficient to account qualitatively for the features in the spectra of the

Ba- and La-based materials.

The photocurrent is proportional to the spectral density:

$$\rho(e)=\frac{1}{\pi}\mathrm{Im}\langle\phi_0|\psi_c^\dagger[e-i\delta-E_0+H(N-1)\psi_c]\phi_0\rangle$$
$$=\frac{1}{\pi}\mathrm{Im}g(e-i\delta)\ .$$

E_0 denotes the ground-state energy neglecting f^1 admixture. The Green's function has the form[23]

$$g(z)=\frac{1}{z-N_f\tilde{\Gamma}(z)}\ ,$$

with

$$\tilde{\Gamma}(z)=\int_{-B}^{0}\frac{V^2(\epsilon)d\epsilon}{z+\epsilon_f-U_{fc}-\epsilon}\ .$$

V is the hybridization matrix element defined by the hybridization parameter $\Delta=\pi\max[V^2(\epsilon)]$, ϵ_f is the energy of the f level and U_{fc} is the f electron–core-hole attraction. The core spectrum shows two characteristic features which become a prominent two-peak structure for the insulating La compounds. These two structures are due to the two poles at $\epsilon=N_F\tilde{\Gamma}(\epsilon)$ of g always present for a rectangular band (of finite width) or for sufficiently strong hybridization. The pole strength is equal to the weight of the f^0 configuration in the final state:

$$\left[1-N_f\frac{\partial}{\partial z}\tilde{\Gamma}(z)\bigg|_{z=N_f\tilde{\Gamma}(z)}\right]^{-1}=W(f^0)\ ,$$

where the ground state is further simplified to $\phi_0|0\rangle$. In the case where one of the poles has considerably more weight than the other, it is justifiable to label the larger peak f^0 and the other f^1. We note that in such a case the separation in the $\Delta\to0$ limit (where the f^1 peak intensity vanishes), is of the order of $\epsilon_f-U_{fc}\sim3$ eV in a metal. In the case of some insulating La compounds such as La_2O_3 where the two peaks are of similar strength, it does not make much sense to label the peaks f^0 and f^1. The labels would have to be interchanged for a small variation of the system parameters. In this case where $\epsilon_f-U_{fc}\sim0$ eV, the two peaks are both of strongly mixed character. Their separation gives a rather direct measure of the hybridization strength Δ. The minimal energy separation of the two poles Δ_{pp} is given for a rectangular band by

$$\Delta_{pp}=2N_f\frac{\Delta}{\pi}\ln\left[\frac{\Delta_{pp}+B}{\Delta_{pp}-B}\right]\ .$$

In the zero-bandwidth limit $B\to0$ with $B\Delta=$const, comparison can be made with the ligand-field cluster model.[29] In this limit the minimal peak separation is $\Delta_{pp}^2=4N_f\Delta B/\pi$; further simplification in the ligand field model with one ligand orbital yields $\Delta_{pp}=2V_{\mathrm{LF}}$. On this basis our $N_f\Delta$ of ~5 eV is comparable to $V_{\mathrm{LF}}\sim2.4$ eV. For finite bandwidth B the impurity model has a continuum contribution to the core XPS spectrum at energies between the two peaks. For a rectangular band the continuum part is

$$\rho(e)_{\delta\to0}=\frac{N_f\Delta}{[e-N_f\Delta\ln(|e+\epsilon_f-U_{fc}+B|/|e+\epsilon_f-U_{fc}|)]^2+\pi^2(N_f\Delta)^2}\quad\text{for}\quad U_{fc}-\epsilon_f-B<e<U_{fc}-\epsilon_f\ .$$

An indication for this contribution can be recognized in the experimental XPS core spectra of La_2O_3 shown in Fig. 2(b), where the "excessive intensity" between the two peaks gives rise to the characteristic tails of the two structures.

[1]T. A. Carlson, M. O. Krause, and W. E. Moddeman, J. Phys. (Paris) Colloq. 32, C4-76 (1971), and references therein.

[2]G. K. Wertheim and A. Rosencwaig, Phys. Rev. Lett. 26, 1179 (1971).

[3]A. Rosencwaig, G. K. Wertheim, and H. J. Guggenheim, Phys. Rev. Lett. 27, 479 (1971).

[4]C. K. Jørgensen and H. Berthou, Chem. Phys. Lett. 13, 186 (1972).

[5]G. K. Wertheim, R. L. Cohen, A. Rosencwaig, and H. J. Guggenheim, in *Electron Spectroscopy*, edited by D. A. Shirley (North-Holland, 1972), p. 813.

[6]A. Signorelli and R. G. Hayes, Phys. Rev. B 8, 81 (1973).

[7]S. Suzuki, T. Ishii, and T. Sagawa, J. Phys. Soc. Jpn. 37, 1334 (1974).

[8]S. Hüfner, in *Photoemission in Solids II*, Vol. 27 of *Topics in Applied Physics*, edited by L. Ley and M. Cardona (Springer, New York, 1978), p. 173.

[9]C. K. Jørgensen, Struct. Bonding (Berlin) 13, 199 (1973); 24, 1 (1975).

[10]B. W. Veal and A. Paulikas, Phys. Rev. Lett. 51, 1995 (1983); Phys. Rev. B 31, 5399 (1985).

[11]D. F. Mullica, C. K. C. Lok, H. O. Perkins, and V. Young, Phys. Rev. B 31, 4039 (1985).

[12]Y. Baer, in *Handbook on the Physics and Chemistry of the Actinides*, edited by A. J. Freeman and G. Lander (North-Holland, Amsterdam, 1984), p. 271.

[13]W. D. Schneider and C. Laubschat, Phys. Rev. Lett. 46, 1023 (1981).

[14]J. F. Herbst and J. W. Wilkins, Phys. Rev. Lett. 43, 1760 (1979).

[15]A. Kotani and J. Toyozawa, J. Phys. Soc. Jpn. 35, 1073 (1973); 35, 1082 (1973); 37, 912 (1974).

[16]A. Kotani, Jpn. J. Phys. 46, 488 (1979).

[17]K. Schönhammer and O. Gunnarsson, Solid State Commun. 23, 691 (1977); 26, 147 (1978); 26, 399 (1978); Z. Phys. B 30, 297 (1978).

[18]R. Manne and T. Åberg, Chem. Phys. Lett. 7, 282 (1970).

[19]P. Burroughs, A. Hamnett, A. F. Orchard, and G. Thornton,

J. Chem. Soc. Dalton Trans. 17, 1686 (1976).
[20]G. Crecelius, G. K. Wertheim, and D. N. E. Buchanan, Phys. Rev. B 18, 6519 (1978).
[21]J. C. Fuggle, M. Campagna, Z. Zolnierek, R. Lässer, and A. Platau, Phys. Rev. Lett. 45, 1597 (1980).
[22]S. J. Oh and S. Doniach, Phys. Rev. B 26, 2085 (1982).
[23]O. Gunnarsson and K. Schönhammer, Phys. Rev. Lett. 50, 604 (1983); Phys. Rev. B 28, 4315 (1983).
[24]J. C. Fuggle, F. U. Hillebrecht, J.-M. Esteva, R. C. Karnatak, O. Gunnarsson, and K. Schönhammer, Phys. Rev. B 27, 4637 (1983).
[25]J. C. Fuggle, F. U. Hillebrecht, Z. Zolnierek, R. Lässer, Ch. Freiburg, O. Gunnarsson, and K. Schönhammer, Phys. Rev. B 27, 7330 (1983).
[26]F. U. Hillebrecht, J. C. Fuggle, G. A. Sawatzky, M. Campagna, O. Gunnarsson, and K. Schönhammer, Phys. Rev. B 30, 1777 (1984).
[27]E. Wuilloud, H. R. Moser, W.-D. Schneider, and Y. Baer, Phys. Rev. B 28, 7354 (1983).
[28]E. Wuilloud, W.-D. Schneider, B. Delley, Y. Baer, and F. Hulliger, J. Phys. C 17, 4799 (1984).
[29]A. Fujimori, Phys. Rev. B 28, 2281 (1983).
[30]S. Hüfner and P. Steiner (unpublished).
[31]G. K. Wertheim, in *Valence Fluctuations in Solids,* edited by L. M. Falicov, W. Hanke, and M. B. Maple (North-Holland, Amsterdam, 1981), p. 67.
[32]F. Riehle, Jpn. Journal of Appl. Phys. 17, Suppl. 17-2, 314 (1978).
[33]J. Kanski and G. Wendin, Phys. Rev. B 24, 4977 (1981).
[34]S. Sato, J. Phys. Soc. Jpn. 41, 913 (1976).
[35]P. Motais, E. Belin, and C. Bonelle, Phys. Rev. B 30, 4399 (1984).
[36]N. Mårtensson, B. Reihl, and R. D. Parks, Solid State Commun. 41, 573 (1982).
[37]H. R. Moser, B. Delley, W.-D. Schneider, and Y. Baer, Phys. Rev. B 29, 2947 (1984).
[38]J. K. Lang, Y. Baer, and P. A. Cox, J. Phys. F 11, 121 (1981).
[39]E. Wuilloud, B. Delley, W.-D. Schneider, and Y. Baer, Phys. Rev. Lett. 53, 202 (1984); 53, 2519 (1984).
[40]Y. Baer and Ch. Zürcher, Phys. Rev. Lett. 39, 956 (1977).
[41]E. Wuilloud, B. Delley, W.-D. Schneider, and Y. Baer, J. Magn. Magn. Mater. 47-48, 197 (1985).
[42]J. K. Lang and Y. Baer, Rev. Sci. Instrum. 50, 221 (1979).
[43]B. Delley and H. Beck, J. Magn. Magn. Mater. 47—48, 269 (1985).
[44]B. Delley and H. Beck, J. Phys. C 17, 4971 (1984).
[45]D. D. Koelling, A. M. Boring, and J. H. Wood, Solid State Commun. 47, 227 (1983).
[46]K. R. Bauchspies, W. Boksch, E. Holland-Moritz, H. Launois, R. Pott, and D. Wohlleben, in *Valence Fluctuations in Solids,* Ref. 31, p. 147.
[47]P. Wachter, in *Valence Instabilities,* edited by P. Wachter and H. Boppart (North-Holland, Amsterdam, 1982), p. 145.
[48]C. M. Varma, Rev. Mod. Phys. 48, 219 (1976).
[49]L. Ley, N. Mårtensson, and J. Azoulay, Phys. Rev. Lett. 45, 1516 (1980).
[50]W. Gordy and W. J. O. Thomas, J. Chem. Phys. 24, 439 (1955).
[51]D. D. Koelling, Physica (Utrecht) 130B, 135 (1985).
[52]Similar data can be found in Refs. 25 and 26.
[53]M. S. S. Brooks, J. Magn. Magn. Mater. 47-48, 260 (1985).
[54]M. R. Norman, D. D. Koelling, A. J. Freeman, H. J. F. Jansen, B. I. Min, T. Oguchi, and Ling Ye, Phys. Rev. Lett. 53, 1673 (1984); M. R. Norman, D. D. Koelling, and A. J. Freeman, Phys. Rev. B 31, 6251 (1985).
[55]F. P. Netzer, G. Strasser, and J. A. D. Matthew, Phys. Rev. Lett. 51, 211 (1983).
[56]J. A. D. Matthew, G. Strasser, and F. P. Netzer, Phys. Rev. B 27, 5839 (1983).
[57]G. Kaindl, G. Kalkowski, W. D. Brewer, E. V. Sampathkumaran, F. Holzberg, A. Schach, and V. Wittenau, J. Magn. Magn. Mater. 47-48, 181 (1985).
[58]C. N. R. Rao, D. D. Sarma, P. R. Sarode, R. Vijayaharaghavan, S. K. Dhar, and S. K. Malik, J. Phys. C 14, 451 (1981).
[59]R. D. Parks, S. Raen, M. L. den Boer, V. Murgai, and T. Mihalisin, Phys. Rev. B 28, 3556 (1983).
[60]S. Raen, M. L. den Boer, V. Murgai, and R. D. Parks, Phys. Rev. B 27, 5139 (1983).
[61]E. Beaurepaire, G. Krill, J. P. Kappler, and J. Röhler, Solid State Commun. 49, 65 (1984).
[62]D. Wohlleben and J. Röhler, J. Appl. Phys. 55, 1904 (1984).
[63]E. V. Sampathkumaran, K. H. Frank, G. Kalkowski, G. Kaindl, M. Domke, and G. Wortmann, Phys. Rev. B 29, 5702 (1984).
[64]J. Röhler, J. Magn. Magn. Mater. 47-48, 175 (1985).
[65]H. Jhans and M. Croft, J. Magn. Magn. Mater. 47-48, 203 (1985).